THE MINERALOGICAL MAGAZINE
AND
JOURNAL OF
THE MINERALOGICAL SOCIETY

No. 241 June, 1958 Vol. XXXI

Bonchevite, $PbBi_4S_7$, a new mineral.

By Ivan Kostov, D.I.C., F.G.S.
Professor of Mineralogy, University of Sofia.

[Read 27 March 1958.]

Summary. In quartz-scheelite veins traversing rocks from the metamorphic complex in the Central Rhodopian mountains, a mineral was found closely resembling bismuthinite. Its composition is Bi 66·62 %, Pb 15·50 %, Cu 0·85 %, and S 16·71 %, corresponding to the formula $PbBi_4S_7$. It is orthorhombic, long prismatic to acicular with an axial ratio $a:b:c = 0{\cdot}9004:1:0{\cdot}3249$. Observed forms: {110}, {100}, {010}, and {011}. Sp. gr. 6·92. Hardness about $2\frac{1}{2}$. Displays a perfect cleavage along {100}. It is distinctly anisotropic. Strongest X-ray intensities: 3·50 Å. (10), 3·08 (8), 1·939 (8), 2·78 (6), 1·733 (6), 2·50 (5). The name is after the eminent Bulgarian mineralogist and petrographer G. Bonchev.

DURING a field practice carried out with students in the Central Rhodopian mountains in 1952, a mineral was found that according to some preliminary microchemical tests was thought to be tetradymite. Owing to certain engagements the mineral was not studied until last year when additional material was secured. Detailed investigations proved it a new mineral from the series Bi_2S_3–$PbBi_2S_4$, to which was given the name *bonchevite* in honour of Academician Georghi Bonchev (Г. Бончев), former professor and founder of the Institute of Mineralogy and Petrography at the University of Sofia.

The mineral occurs in quartz veins cutting a metamorphic rock series, mainly gneisses and amphibolites, of unknown age, in close proximity to the so-called Yugovo granite. The latter is considered to be of Tertiary age. The mineral paragenesis includes as principal minerals scheelite, pyrite, and bonchevite with sparse zincblende and molybdenite. The gangue is exclusively milky quartz, locally enriched in calcite. White mica often develops along the selvages of the veins.

Morphology. The new mineral is found usually as acicular or lon prismatic crystals and aggregates up to 2 cm. in size. Most of them ar tectonically deformed (fig. 1). The crystals are apparently orthorhombic On four crystals measured with the reflection goniometer angles of 48 and 18° were observed, corresponding to ϕ for $m\{110\}$ and ρ for $e\{011$

Fig. 1. Fig. 2.

Fig. 1. Bonchevite crystals in milky quartz. ×20.
Fig. 2. Typical habit of bonchevite.

respectively. In addition the forms $a\{100\}$ and $b\{010\}$ have been recog nized. Observed combinations were: {110}{011}, {110}{100}{011} (fig. 2 and {110}{100}{010}{011}. The axial ratio as determined from the abov angles is $a:b:c = 0{\cdot}9004:1:0{\cdot}3249$, which lies between those for bi muthinite (0·9862:1:0·3498) and galenobismutite (0·8050:1:0·2828 The faces {110} are commonly striated along the *c*-axis.

Physical properties. A perfect cleavage apparently along {100} observed on most crystals. Otherwise the mineral shows an uneven subconchoidal fracture; the crystals are very brittle. Hardness about 2 The density was determined on five samples using the method suggeste by N. I. Rudenko and M. M. Vassilevski (1957); the mean value thu obtained is 6·92. The mineral is lead- to steely-grey with metallic lustr

in polished sections it is weakly pleochroic and distinctly to strongly anisotropic. Several polished sections etched with HCl, HNO_3, and $FeCl_3$ failed to reveal any inhomogeneities (fig. 3). Very sporadic minute inclusions, most probably of native bismuth, are found in some sections.

Chemical composition. Carefully selected samples of the mineral have been analysed by N. Yordanov, Senior Assistant in Analytical Chemistry

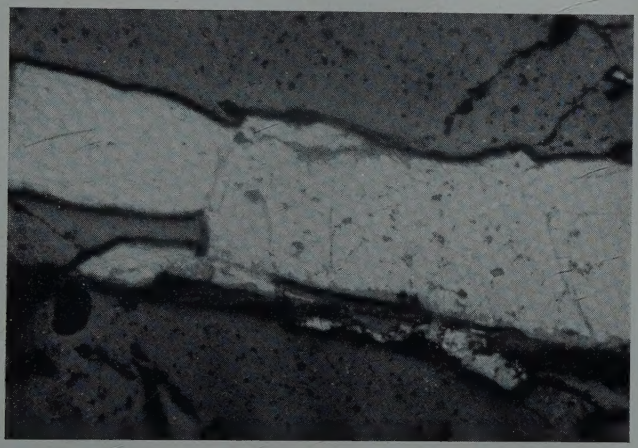

FIG. 3. Polished section of bonchevite showing cleavage and rims of weathered products. ×150.

in the University of Sofia, firstly by using the polarograph in order to get a provisional idea about its composition and then by a tested analytical procedure in order to secure a complete separation of the bismuth from the lead. The results in all cases closely agreed. The complete analysis of the mineral gave the following percentages: Bi 66·62 %, Pb 15·50 %, Cu 0·85 %, S 16·71 %, total 99·68 %. The analysis corresponds almost exactly to the ideal formula $2Bi_2S_3.PbS$ or $PbBi_4S_7$. Apart from lead, bismuth, copper, and sulphur, Ag, Zn, Cd, Sb, and Te have been detected spectrographically; the last element was also found by micro-chemical tests.

Rims of a weathering product, probably a bismuth carbonate, are found around some of the bonchevite crystals (fig. 3).

X-ray diffraction data. Powder patterns of bonchevite were recorded using a VEM 'TUR' M 60 apparatus and standard camera with copper radiation and nickel filter. All patterns proved to be identical. X-ray powder data of the best diffraction photograph are given in table I

(fig. 4) together with X-ray powder data of related minerals. Th intensities are estimated visually.

The X-ray powder pattern of bonchevite is very similar to but no identical with that of the bismuthinite. As the only X-ray data o bismuthinite to hand were those by A. Harcourt (1942), several selecte

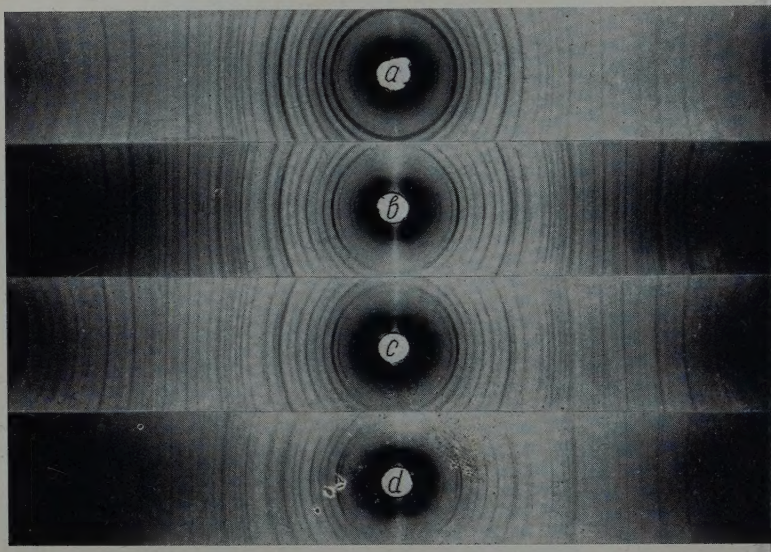

FIG. 4. X-ray powder photographs of bonchevite (*a*); bismuthinite from Tele marken, Norway (*b*); bismuthinite from Cerro de Chorolque, Bolivia (*c*); an galenobismutite from Falun, Sweden (*d*).

samples from two rich specimens from the mineral collection of th University of Sofia have been X-rayed for comparison, one labelle Bleka, Telemarken, Norway, the other Mina Coronacion, Cerro d Horolque, Bolivia. Semiquantitative spectrographic analyses of thes bismuthinites revealed less than 1 % Pb. Their X-ray powder pattern are identical (see table I and fig. 4 *b* and *c*), but are different from tha of the bismuthinite given by Harcourt. On the other hand, the X-ra patterns of the Norwegian and Bolivian bismuthinites differ distinctl from that of the bonchevite in the intensities and slight changes of th *d*-values of some lines. Thus:

bonchevite: d = 3·50 (10), 3·08 (8), 2·78 (6), 2·50 Å. (5).
bismuthinite: Norway: d = 3·44 (10), 3·03 (5), 2·76 (3), 2·48 Å. (7).
Bolivia: d = 3·46 (10), 3·06 (5), 2·76 (3), 2·47 Å. (7).

In addition there is the line 3·70 Å. in the powder pattern of bonchevite, lacking altogether in the X-ray patterns of the bismuthinites. This value is, however, met with in the X-ray powder data of galenobismutite as given by L. G. Berry (1940). Another specimen of galenobismutite from Falun, Sweden, X-rayed by the author for comparison, showed *d*-values agreeing well with those given by Berry (see table I). The differences between these X-ray patterns and that of bonchevite are, however, obvious. Having in mind the internal homogeneity of the crystals of the new mineral and the differences displayed by its X-ray patterns and crystallography it is logical to assume a new phase in the system Bi_2S_3–$PbBi_2S_4$ rather than a mixture of these two 'end-members'.

Discussion. The system Pb–Bi–S was recently dealt with by A. R. Graham, R. M. Thompson, and L. G. Berry (1953) who obtained by hydrosynthetic experiments Bi_2S_3, galenobismutite, PbS, and phase 2 = cannizzarite, redefining the latter as a mineral species on X-ray grounds, without giving for it any formula. Cannizzarite was described from the fumaroles on Vulcano, Lipari Islands, by Zambonini, de Fiore, and Carobbi (1925), who gave for it the formula $PbBi_4S_7$, the same as that of bonchevite. In a revision of the chemical composition of cannizzarite Wolfe (1938) gives a formula $Pb_3Bi_5S_{11}$ and axial ratio $a:b:c$ = 0·8050:1:0·2828. The latter, according to M. A. Peacock (Dana, 1944), corresponds to the axial ratio of galenobismutite and in Dana's 'Mineralogy' (7th edn) cannizzarite is considered to be identical with galenobismutite. It should be noted also that Wolfe's formula is with uncompensated charges, showing an excess of sulphur. As Carobbi's analysis agrees well with the composition of bonchevite it is possible that the specimens studied by Zambonini differed from those described by Wolfe and that the originally described cannizzarite was in fact identical with the mineral dealt with in this paper. The name cannizzarite as re-established by Graham, Thompson, and Berry refers, however, to a product which has an entirely different X-ray pattern, similar to that of the mineral X-rayed by Harcourt (see table I). This mineral (Harcourt's cannizzarite) again comes from the Lipari Islands.

Three more minerals have already been described in the series Bi_2S_3–$PbBi_2S_4$: ustarasite, $PbBi_6S_{10}$ (Saharova, 1955), chiviatite, $Pb_3Bi_8S_{15}$ (Rammelsberg, 1853), and rezbanyite, $Pb_4Bi_{10}S_{19}$ (Frenzel, 1883). For rezbanyite the formulae $Pb_2Bi_6S_{11}$ and $Cu_2Pb_3Bi_{10}S_{19}$ have also been suggested (Ramdohr, 1955; Koch, 1948; Padera, 1956), the last mentioned perhaps more becoming so far as the type mineral is concerned. The remaining two minerals are not firmly established as

TABLE I. X-ray powder diffraction data for bonchevite and related minerals.

Bonchevite Rhodopian Mts.		Bismuthinite Harcourt, 1942		Bismuthinite Norway		Bismuthinite Bolivia		Ustarasite Sakharova, 1955		Galeno-bismutite Sweden		Galeno-bismutite Berry, 1940		Cannizzarite Harcourt, 1942		Cannizzarite Graham, Thompson, Berry, 1953	
d, Å.	*I.*	*d*, Å.	*I.*	*d*, Å.	*I.*	*d*, Å.	*I.*	*d*, Å.	*I.*	*d*, Å.	*I.*	*d*, Å.	*I.*	*d*, Å.	*I.*	*d*, Å.	*I.*
5·42	2	5·55	1·0	5·38	2	5·45	2	5·524	w	5·50	3	—	—	—	—	7·38	1
4·93	2	4·95	1·0	4·90	2	4·87	2	4·895	w	4·90	3	—	—	—	—	5·13	2
4·16	1	—	—	—	—	—	—	—	—	—	—	—	—	—	—	—	—
3·87	2	3·92	2·0	3·83	3	3·83	4	3·885	m	—	—	—	—	3·80	3·0	3·82	10
3·70	2	—	—	—	—	—	—	—	—	3·70	5	3·67	w	—	—	—	—
3·50	10	3·50	9·0	3·50	1	—	—	3·527	vs	—	—	—	—	3·51	1·0	3·49	3
—	—	—	—	3·44	10	3·46	10	3·382	m	3·48	10	3·47	vvs	3·35	1·0	3·38	3
3·18	1	3·22	1·0	—	—	—	—	—	—	3·14	1	3·25	vw	—	—	3·29	1
3·08	8	3·08	6·0	3·03	5	3·06	5	3·080	s	3·05	3	3·03	s	3·00	3·0	3·01	6
—	—	—	—	—	—	—	—	—	—	—	—	—	—	2·87	2·0	2·87	5
2·78	6	2·79	4·0	2·76	3	2·76	3	2·785	m	2·77	4	2·79	w	2·78	0·3	2·76	2
2·69	1	2·69	1·0	2·68	1	—	—	2·702	w	—	—	2·66	vw	2·68	2·0	2·68	6
2·63	1	2·61	1·0	2·58	1	—	—	2·627	w	2·55	1	—	—	2·56	0·2	2·54	2
2·50	5	2·495	3·0	2·48	7	2·47	7	2·508	s	2·49	8	2·47	vs	—	—	—	—
2·46	1	2·425	1·0	—	—	—	—	2·443	vw	2·44	1	—	—	—	—	—	—
—	—	—	—	—	—	—	—	—	—	—	—	2·38	m	2·37	0·2	2·39	0·5
2·30	1	2·28	1·0	2·27	1	—	—	2·295	w	—	—	2·26	vw	—	—	—	—
2·23	4	2·23	3·0	2·21	4	2·23	4	2·242	m	2·23	6	2·19	vw	2·22	1·0	2·22	5
—	—	—	—	—	—	—	—	—	—	—	—	—	—	—	—	—	—
2·10	2	2·06	0·5	2·07	2	2·08	3	2·073	w	2·09	4	2·06	s	2·03	3·0	2·03	5
—	—	—	—	—	—	—	—	—	—	—	—	2·02	vw	—	—	—	—
1·984	3	1·98	1·0	—	—	—	—	1·980	w	1·969	1	1·975	s	—	—	—	—
—	—	—	—	1·954	1	—	—	—	—	1·929	5	—	—	—	—	—	—
1·939	8	1·935	5·0	—	—	—	—	—	—	—	—	—	—	—	—	—	—
—	—	—	—	1·910	8	1·915	8	1·915	s	—	—	—	—	—	—	1·910	4
—	—	—	—	—	—	—	—	—	—	—	—	1·905	vw	1·90	0·5	—	—
—	—	1·870	1·0	—	—	—	—	1·884	m	1·882	4	1·882	m	—	—	—	—
1·855	1	—	—	1·855	2	—	—	1·857	m	—	—	—	—	—	—	—	—

1·846	1	1·840	1·0	—	—	1·846	3	—	—	1·837	1	—	—	—	—	—	—
—	—	—	—	1·829	1	—	—	—	—	—	—	1·772	s	1·79	1·0	1·791	3
1·778	1	—	—	—	—	—	—	1·732	s	1·726	3	1·729	vw	1·735	0·5	1·734	1
1·733	6	1·725	5·0	1·722	4	1·726	2	1·699	w	1·696	1	1·699	vw	—	—	—	—
—	—	1·690	1·0	—	—	—	—	1·680	w	—	—	—	—	1·68	0·5	1·684	2
1·685	1	—	—	1·685	2	—	—	—	—	—	—	—	—	1·62	0·3	1·618	0·5
—	—	1·670	1·0	—	—	1·677	1	—	—	—	—	—	—	1·58	0·2	1·573	1
1·604	3	1·595	0·2	—	—	—	—	1·556	w	1·546	2	—	—	—	—	—	—
—	—	1·550	3·0	1·540	3	—	—	1·532	w	1·527	2	—	—	—	—	1·526	0·5
1·536	1	1·521	0·5	1·521	1	1·534	1	—	—	1·516	4	1·510	vw	—	—	—	—
—	—	—	—	—	—	—	—	1·483	vs	—	—	—	—	1·482	0·2	1·488	1
1·478	3	1·475	2·0	1·472	6	1·472	4	1·442	m	1·444	2	1·451	m	1·435	0·2	1·441	0·5
1·440	3	1·430	2·0	—	—	—	—	1·429	m	—	—	—	—	—	—	—	—
—	—	—	—	1·426	2	1·426	3	—	—	—	—	1·415	m	—	—	—	—
—	—	—	—	—	—	—	—	1·400	m	—	—	—	—	—	—	—	—
—	—	—	—	1·408	2	—	—	1·384	vw	1·392	2	—	—	1·385	0·2	1·384	1
1·389	2	1·390	1·0	—	—	1·385	1	—	—	—	—	1·378	m	—	—	—	—
—	—	1·375	1·0	—	—	—	—	1·352	m	1·353	3	—	—	1·355	0·2	—	—
1·350	2	1·347	2·0	1·341	4	1·344	2	—	—	1·323	2	—	—	1·320	0·2	1·326	1
—	—	1·315	1·0	—	—	1·312	3	—	—	—	—	—	—	—	—	—	—
1·309	4	—	—	1·309	2	—	—	1·308	m	1·305	3	—	—	—	—	—	—
—	—	1·302	2·0	1·303	3	—	—	1·296	w	—	—	—	—	1·295	0·3	1·295	1
—	—	1·289	0·5	—	—	—	—	1·283	w	—	—	—	—	—	—	1·274	0·5
—	—	1·275	0·5	—	—	—	—	—	—	—	—	—	—	1·265	0·2	—	—
1·250	1	—	—	—	—	1·256	1	—	—	1·254	2	—	—	1·228	0·3	1·232	0·5
—	—	1·242	0·5	1·240	3	1·242	2	1·247	w	—	—	—	—	1·205	0·3	—	—
1·218	1	1·184	2·0	1·180	3	1·181	2	1·189	m	—	—	—	—	—	—	1·172	2
—	—	1·160	0·5	1·161	1	1·158	1	1·166	w	—	—	—	—	1·168	0·3	—	—
1·142	4	1·138	2·0	1·136	4	—	—	1·140	s	1·147	1	—	—	1·145	0·3	—	—
—	—	1·116	0·5	1·119	1	—	—	1·110	m	1·134	1	—	—	1·130	0·2	—	—
1·103	1	—	—	—	—	—	—	1·102	m	1·109	1	—	—	1·075	0·2	—	—
—	—	1·096	0·3	1·089	3	—	—	1·057	vs	—	—	—	—	1·050	0·2	—	—

definite species. With the rational ratio Bi_2S_3:PbS = 2:1, one could accept logically the mineral described in this paper as a well-defined new intermediate but not isomorphous member of the series Bi_2S_3–$PbBi_2S_4$ (Kostov, 1957).

Acknowledgements. The author is indebted to Dr. K. Padera of the Karlovy University, Prague, for supplying provisional X-ray powder data of the new mineral and for helpful suggestions. Thanks are due also to Ing. A. Papazov, of the Institute of Metallurgy, for additional powder diagrams. To N. Yordanov, Senior Assistant in Analytical Chemistry in the University of Sofia, the author is obliged for the chemical analyses, and to Mrs. Y. Mincheva-Stefanova of the Geological Institute of the Bulgarian Academy of Sciences for the spectrographic work.

References.

Berry (L. G.), 1940. Amer. Min., vol. 25, p. 726 [M.A. **8**–214].

Frenzel (A.), 1883. Tschermaks Min. Petr. Mitt., vol. 5, p. 175.

Graham (A. R.), Thompson (R. M.), and Berry (L. G.), 1953. Amer. Min., vol. 38, p. 536 [M.A. **12**–206].

Harcourt (G. A.), 1942. Ibid., vol. 27, p. 63 [M.A. **8**–280].

Koch (S.), 1930. Centr. Min., Abt. A, p. 49 [M.A. **4**–480].

[Kostov (I.)] Костов (И.), 1957. Зап. Всесоюз. Мин. Общ. [Mem. All-union Min. Soc.], vol. 86, p. 336.

Padera (K.), Bouska (Vl.), and Pelikan (J.), 1955. Chemie der Erde, vol. 17, p. 329.

—— 1956. Ibid., vol. 18, p. 14.

Peacock (M. A.), 1944. Cited in Dana's System of Mineralogy, 7th edn, vol. 1, p. 742.

Ramdohr (P.), 1955. Die Erzmineralien und ihre Verwachsungen, p. 596.

Rammelsberg (C. F.), 1853. Ann. Phys. Chem. (Poggendorff), vol. 88, p. 320.

[Rudenko (N. I.) and Vasilevski (M. M.)] Руденко (Н. И.) и Василевский (М. М.), 1957. Зап. Всесоюз. Мин. Общ. [Mem. All-union Min. Soc.], vol. 86, p. 131.

[Sakharova (M. S.)] Сахарова (М. С.), 1955. Труды Мин. муз. Акад. наук СССР [Proc. Min. Mus. Acad. Sci. USSR], vol. 7, p. 112 [M.A. **13**–164].

Wolfe (C. W.), 1938. Amer. Min., vol. 23, p. 790 [M.A. **7**–386].

Zambonini (F.), De Fiore (O.), and Carobbi (G.), 1925. Rend. Accad. Sci. Fis. Mat. Napoli, ser. 3, vol. 31, p. 24 [M.A. **3**–10].

The infra-red spectra of talc, saponite, and hectorite.

By V. C. Farmer, B.Sc., Ph.D.

The Macaulay Institute for Soil Research, Aberdeen, Scotland.

[Communicated by Dr. R. C. Mackenzie; read 27 March 1958.]

Summary. The absorption spectra of talc, saponite, and hectorite between 4000 and 400 cm.$^{-1}$ are closely related, although the bands of the smectites are more diffuse as a result of isomorphous substitutions in the talc structure. Using oriented specimens, vibrations in which the change of dipole moment is perpendicular to the sheets of the minerals are identified, and the results compared with theoretical predictions. Three bands arising from the stretching vibrations of interlayer water molecules in the smectites are distinguished, one of which corresponds to a very weak hydrogen bond. Spectral changes arising from vigorous grinding are discussed.

THE infra-red spectra of the principal clay minerals have now been broadly surveyed by several workers in the frequency range 4000 to 650 cm.$^{-1}$, the principal compilations being those of Adler *et al.* (1951) and Hunt *et al.* (1950). More recently Beutelspacher (1956 *a*, *b*) has re-examined many of them using improved techniques, and has published well-resolved spectra extending to 400 cm.$^{-1}$. The present situation and some of the outstanding problems awaiting solution have been well summarized by Nahin (1955), and in this paper some of these problems are investigated in the spectra of the trioctahedral minerals based on the talc structure. This group of minerals has received rather less attention than the more common dioctahedral layer minerals based on pyrophyllite. The spectrum of saponite does not appear to have been previously reported. Published spectra of talc and hectorite in the compilations already referred to show some variation, part of which probably arises from the use of oriented specimens by the earlier workers. Variations in the spectra with orientation prove, however, to be of value in correlating a simplified theoretical analysis of the infra-red-active vibrations of talc with its absorption bands. In addition, changes in the spectra associated with the isomorphous substitutions that constitute the difference between talc and the smectites, saponite and hectorite, are discussed, and the influence of the exchangeable ion on the infra-red absorption of the smectites is investigated.

Materials and methods.

The talc used was a pure specimen from Greiner, Tyrol, and the hectorite a type specimen from Hector, California. The saponite, from

Allt Ribhein, Skye, has been characterized by Mackenzie (1957) as of excellent purity, from chemical, thermal, and X-ray data. The spectra were recorded in the region 4000 to 650 cm.$^{-1}$, on a Grubb Parsons S4 double-beam infra-red spectrometer equipped with sodium chloride prism, and in the region 650 to 400 cm.$^{-1}$ on a Hilger H800 double-beam spectrometer, using a potassium bromide prism. Calibration was by the usual standards (Downie *et al.*, 1953) and was accurate to within 3 cm.$^{-1}$ below 1700 cm.$^{-1}$ and to about $\pm$10 cm.$^{-1}$ at 3700 cm.$^{-1}$.

Samples were generally examined in potassium bromide pressed disks, using equipment already described (Farmer, 1956), but oriented films, whose preparation is described below, were also used. Whilst the pressed-disk technique gives excellent spectra of silicates, it is less satisfactory in studying the infra-red absorption of interlayer water in smectites, as the degree of hydration is not easily controlled. Pressed disks generally show bands due to water adsorbed on the potassium bromide particles, but this interference can be reduced to relatively low levels if the grinding time is not too long and if a compensating blank is used. At high humidities some replacement of the exchangeable ion by potassium from the bromide is to be expected, so the two smectites were examined at humidities below 50 % immediately after preparing the disks. Pressed disks are sufficiently porous to permit smectites dispersed in them to be dehydrated by heating the disks to 200° C., so changes in the spectra associated with loss of almost all the interlayer water are readily followed. The process is reversible, and dehydrated smectites in pressed disks rapidly take up water from the atmosphere. This observation may go some way to explain the results of Roy and Roy (1957), who found that clays that had been dehydrated or exposed to D_2O still showed the bands that are generally assigned to interlayer and adsorbed H_2O.

Orientation effects in the preparation of clay samples.

Excellent spectra of clays (e.g. Beutelspacher, 1956 *a*, *b*) can be obtained by the pressed-disk technique: a small vibratory grinder is used to grind and mix the sample with excess potassium bromide from which a transparent disk is formed under pressure. The spectra show little scattering even at 4000 cm.$^{-1}$, due to the small particle size achieved and to the similar refractive indices of sample and surrounding medium. Before the introduction of this convenient method, good spectra showing little scattering below 1700 cm.$^{-1}$ had been obtained by evaporating clays dispersed in *iso*-propyl alcohol on to sodium chloride windows

(Hunt and Turner, 1953) or aqueous suspensions on to silver chloride sheet (Adler and Kerr, 1951; Nahin *et al.*, 1951). It is common practice, however, to obtain partially oriented specimens for X-ray studies by deposition from suspension, and it seemed likely that such deposits would give spectra showing orientation effects, as radiation passing

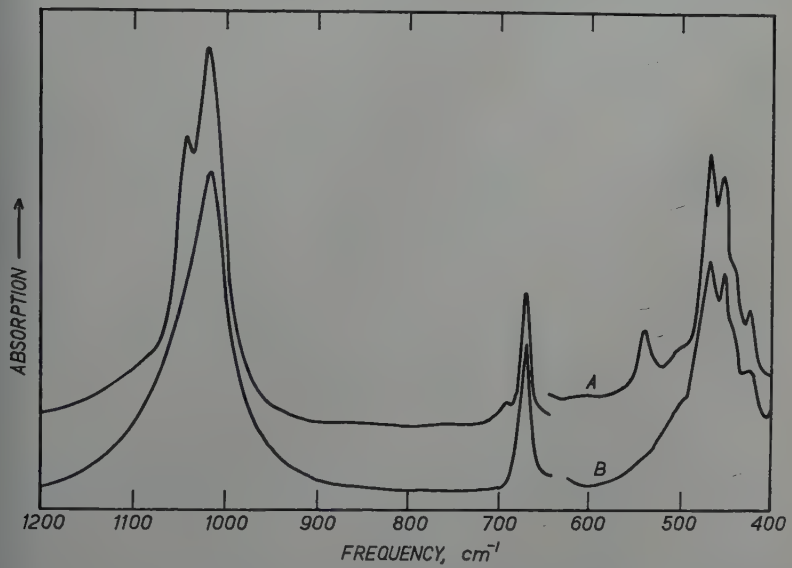

FIG. 1. Infra-red absorption of talc. A, pressed disk, sample concentration about 0·08 mg./cm.²; B, oriented deposit on KBr window.

perpendicularly through clay sheets can only excite dipole moment oscillations with a component parallel to the sheet. A comparison of published spectra proved difficult because of variations in concentration and origin of sample and in the performance of spectrometers. A strict comparison has now been made on one instrument, which leaves little doubt that the effect can occur.

In preparing the oriented specimens, a modification of the technique described by Hunt and Turner (1953) was used. In place of their cyclonic disintegrator, a vibratory grinder of the Ardenne (1941) type was used to reduce particle size. The vibrator, which is developed from a design of Ford, Wilkinson, and Price (1954), has already been described (Farmer, 1956). In preliminary experiments it was noted that after grinding alone for 10 minutes the spectra of talc and saponite were considerably modified (fig. 7). This effect will be discussed more fully later.

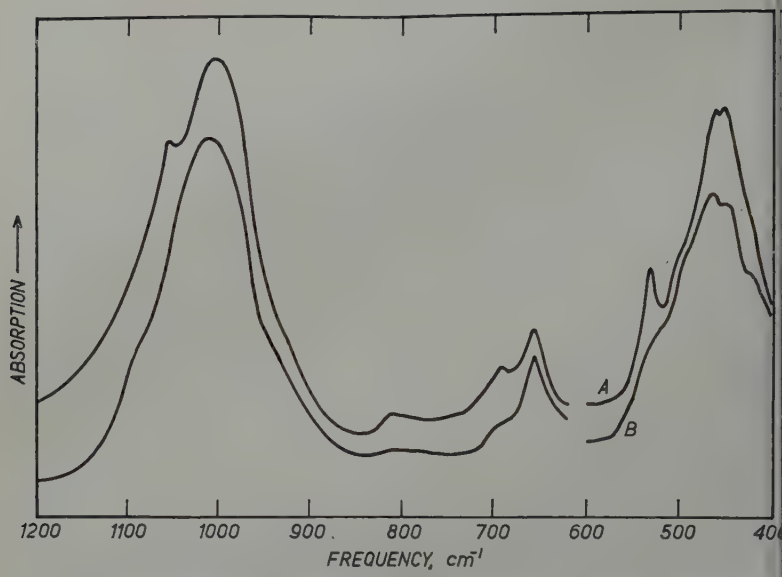

FIG. 2. Infra-red absorption of saponite (Ca^{++} saturated). A, pressed disk, sample concentration about 0·25 mg./cm.^{2}; B, oriented deposit on KBr window.

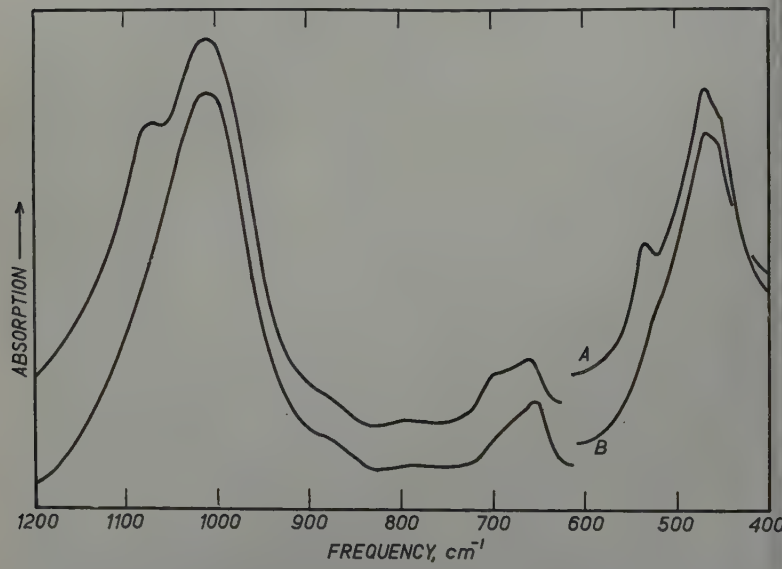

FIG. 3. Infra-red absorption of hectorite (natural). A, pressed disk, sample concentration about 0·3 mg./cm.^{2}; B, oriented deposit on KBr window.

Little change in the spectra occurred during the preparation of potassium bromide disks even after 10 minutes' grinding, but here the excess potassium bromide would be expected to have a cushioning effect.

Similarly, no spectral changes occurred when the minerals were ground in the presence of *iso*-propyl alcohol, and the resulting dispersion gave satisfactory deposits of the smectites. 15 mg. of the mineral (< 200 mesh) together with 0·5 ml. *iso*-propyl alcohol and three ball-bearings were placed in a stainless steel capsule fitted with a polythene stopper, which was then shaken at 100 cycles/sec. in the vibratory grinder for 2 minutes. A few drops of the suspension placed on a potassium bromide plate were then spread and stirred with a fine wire until the suspension gelled. Evaporation then gave a uniform deposit. In preparing deposits of talc, it was found necessary first to grind this mineral alone in the vibratory grinder for 1 minute; *iso*-propyl alcohol was then added and the above procedure followed. An X-ray examination of the hectorite and saponite deposits in the region of their 001 reflections showed them to be well oriented, and it is to be expected that in infra-red absorption measurements refraction of the radiation would improve the effective orientation by bending the beam nearer to the normal to the sheets.

Spectra obtained from such deposits are compared with those from pressed disks for talc (fig. 1), saponite (fig. 2), and hectorite (fig. 3). It will be seen that both types of preparation show strong or very strong absorption near 1010, 660, and 460 cm.$^{-1}$. Bands shown by the pressed disks near 1050, 690, and 530 cm.$^{-1}$, however, are weak or absent in the spectra of the deposits, and so can safely be assigned to vibrations in which the dipole change is perpendicular to the sheets. The frequencies of the absorption bands of these minerals are listed in table I, which includes weaker bands only detectable at higher concentrations than those used for the reproduced spectra. The assignment of those bands that arise from vibrations involving Si–O and Mg–O vibrations (below 1100 cm.$^{-1}$) will be discussed in the following section. The structural hydroxyl group of these minerals and the interlayer water of the smectites have stretching vibrations between 3000 and 3700 cm.$^{-1}$, and these will be treated separately.

Correlation of structure and spectra.

Talc. The spectra of the three trioctahedral minerals reflect the close relationship between them, and it is clear that an interpretation of the better-defined spectrum of talc would lead to an assignment of the

principal bands of the smectites. A full analysis of the normal vibrations of the talc structure is, however, formidable. The mineral consists of magnesium silicate sheets of indefinite extent (Bragg, 1937). The forces within the sheets are largely electrostatic, but between sheets only weak van der Waals forces act. The unit cell, point group C_{2h}, contains two

TABLE I. Frequencies (cm.$^{-1}$) of infra-red absorption bands of the magnesium silicate sheets of talc, saponite, and hectorite.

Assignment.	Talc.	Saponite.	Hectorite.†
ν_4+(OH)$^-$ str.	4330 vvw	4330 vvw	4330 vvw
ν_6+(OH)$^-$ str.	4200 vvw		
(OH)$^-$ str.	3670 w	3697 w 3670 w	3670 w 3610 w
summation bands	1919 vvw 1866 vvw 1818 vvw 1770 vvw 1706 vvw		
Si–O ν_1 ⊥	1045 vs	1056 vs	1073 vs
Si–O ν_3 ∥	1018 vs	1005 vs	1011 vs
		809 w	799 w
	783 w	784 infl.	
		737 infl.	
Si–O ν_2 ⊥	690 m	692 m	696 m
Si–O ν_4 ∥	670 s	655 m	655 m
Mg–O ν_6 ⊥	539 m	534 m	533 m
	500 infl.	490 infl.	
Mg–O ν_7 ∥	467 vs 452 vs	464 vs 450 vs	465 vs
	444 infl.		
Si–O ν_5 ∥	426 m	420 w	

† The spectrum given by Beutelspacher (1956) shows absorption bands at 1430 and 880 cm.$^{-1}$ due to a calcite impurity.

w, weak; m, medium; s, strong; v, very; infl., inflexion.

units of empirical formula $Mg_3Si_4O_{10}(OH)_2$ from separate sheets, giving 123 normal vibrations, about half of which can be infra-red-active, the remainder being Raman-active. The infra-red-active vibrations fall into two classes, one of symmetry A_u in which the change in dipole moment is along the *b*-axis, which lies in the plane of the sheets, the other of symmetry B_u in which the dipole moment changes perpendicularly to this axis, so that none need be perpendicular to the plane of the sheets. The presence of perpendicularly polarized bands, together with the relative simplicity of the spectrum, suggests, however, that the spectrum can be interpreted in terms of the marked pseudo-hexagonal

symmetry of talc, arising from the hexagonal symmetry of the silicon-oxygen framework. Qualitative arguments support this.

The problem can be simplified by considering an isolated magnesium-silicate sheet, as the weak forces between sheets have little effect on the vibrations in the region investigated here: it is well known, for example,

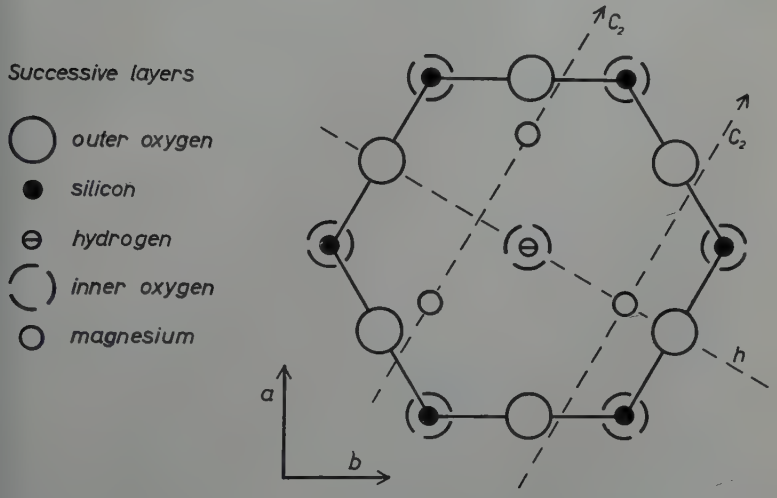

FIG. 4. Single-layer unit cell of talc. Only half of the silicon and oxygen ions are shown, the remainder being obtained by the operation of the twofold axes, C_2, which pass through the magnesium ions.

that the spectra of rigid non-polar organic molecules in the solid state differ little from their solution spectra. Within a single sheet an effective unit cell of symmetry C_{2h} can be distinguished, as in fig. 4. The magnesium ions lie sandwiched between two silicate layers, which are symmetrically related by twofold axes passing through the magnesium ions. For clarity, only one silicate layer is shown in the figure. The twofold axes, C_2, and the plane of symmetry, h, of this unit cell are not symmetry elements of the crystal: their orientation alternates in successive sheets by the operation of the glide planes of the space lattice. The centres of symmetry lying at the intersection of the plane with the axes do, however, persist in the crystal.

A further simplification is possible by treating the vibrations of the silicon-oxygen layers separately from the magnesium vibrations. Certainly the higher-frequency vibrations of talc can involve little motion of the magnesium ions: all silicates show strong absorption near

1000 cm.$^{-1}$ (Launer, 1952) clearly arising from Si–O stretching frequencies, whereas Mg–O vibrations occur round 450 cm.$^{-1}$ in magnesium oxide (Lax and Burstein, 1955). Si–O bending frequencies are less well characterized (Duval and Lecomte, 1954; Matossi and Bronder, 1938) and will certainly vary widely with the particular polysilicate ion involved. Comparison with other XO_4 anions (Hertzberg, 1945) suggests that they probably extend down to at least 400 cm.$^{-1}$, and so are likely to interact with Mg–O vibrations. These considerations make attempts to treat silicate spectra in terms of the vibrations of an isolated SiO_4 tetrahedron unsatisfactory (Weiler, 1932; Matossi and Bronder, 1938).

The silicon-oxygen layers of talc considered as isolated units have hexagonal symmetry (C_{6v}) with the hexagonal axes perpendicular to the sheets. Following the treatment of Mathieu (1945), who gives tables that include some of the special local symmetries that occur in crystals, this structure has only five infra-red active vibrations, two polarized perpendicularly to the sheets (ν_1 and ν_2, class A_1) and three degenerate vibrations in the plane of the sheets (ν_3, ν_4, and ν_5, class E_1). In addition there is one inactive vibration of class B_1, three of class B_2, and three degenerate Raman-active vibrations of class E_2. When integrated into a crystal of symmetry C_{2h}, however, the degenerate vibrations are split, the previously inactive vibrations can absorb radiation, and the form of the vibrations becomes more or less altered. Nevertheless, in talc the perturbing effect of the environment on the Si–O vibrations appears to be small. This can probably be correlated with the fact that the magnesium ions are linked to the silicon-oxygen layers only through the inner layer of oxygen atoms, each of which has three magnesium ions symmetrically disposed about it, so that the symmetry of the force field is largely preserved.

The approximate form of the infra-red-active vibrations for C_{6v} symmetry are shown in fig. 5 in so far as they affect a single silicon-oxygen tetrahedron. Examination of these shows that ν_1 is a pure stretching frequency and so is correlated with the highest-frequency perpendicular vibration at 1045 cm.$^{-1}$. The parallel vibration ν_3 is largely a stretching frequency but necessarily includes a small bending component which agrees well with the slightly lower frequency of the band at 1018 cm.$^{-1}$. Both ν_2 and ν_4 combine stretching and bending motions, and are assigned to the bands at 690 and 670 cm.$^{-1}$ respectively. Vibration ν_5, largely a bending vibration, should be of lowest frequency and so may contribute to the complex absorption band centred on 450 cm.$^{-1}$.

Turning now to the motions of the magnesium ions, it may be noted that the position of these ions in talc, sandwiched between sheets of close-packed oxygens, is similar to their position in brucite, where the oxygens belong to hydroxyl groups (Bragg, 1937). The brucite structure is of higher symmetry, however (D_{3d} with both Mg and OH on threefold

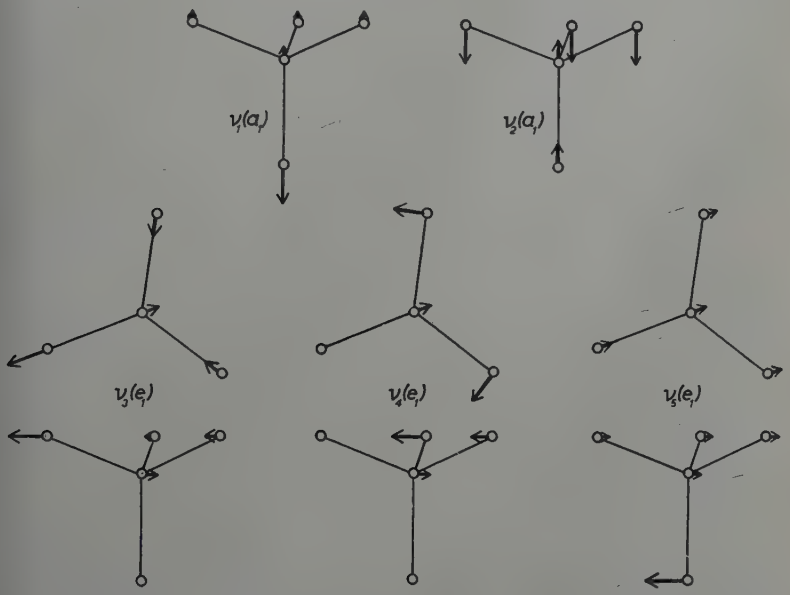

FIG. 5. Approximate form of the infra-red vibrations of silicon-oxygen tetrahedra, when linked in a sheet of symmetry C_{6v}.

axes), for which elementary theory predicts only two infra-red-active vibrations involving magnesium ions, one in which they move perpendicularly to the oxygen sheets, and the other a degenerate vibration parallel to the sheets. Brucite absorbs at 560 and 458 cm.$^{-1}$ (Beutelspacher, 1956*a*) and our own observations indicate that the weaker higher-frequency band corresponds to the perpendicular mode, as it is absent from the spectrum of an oriented film. The only other perpendicular vibration of brucite is an O–H stretching frequency near 3700 cm.$^{-1}$. The band at 458 cm.$^{-1}$ is probably largely due to the degenerate in-plane Mg–O vibrations although the bending frequency of the hydroxyl groups has been predicted to lie near 400 cm.$^{-1}$, and is of the same symmetry type (Hexter and Dows, 1956).

It seems likely that the magnesium ions of talc perform vibrations

similar in type to those of brucite. It is only if the magnesium ions al move in phase, and if their motions are restricted to being either per pendicular or parallel to the sheets, that they can couple with th silicon-oxygen vibrations, already discussed, without perturbing thei form markedly and splitting the degeneracy of the E_1 vibrations. I seems reasonable, then, to assign the band of talc at 539 cm.$^{-1}$ to th perpendicular magnesium vibration, its frequency being rather lowe than that of brucite owing to an increase in the effective mass of th oxygen atoms of talc. Similarly the strong doublet at 452 and 467 cm.$^{-}$ is taken to correspond to the in-plane vibration of brucite at 458 cm.$^{-1}$ with its degeneracy lifted. This vibration should couple strongly wit the vibration ν_5 of the silicate layer, which may be at 426 cm.$^{-1}$.

A stricter analysis shows that the magnesium ions in talc, unlik those of brucite, are not all symmetrically related, one ion in each uni cell being at a site of symmetry C_{2h}, the other two having symmetry C_{2} As a result they contribute six degrees of freedom to the infra-red-activ vibrations of talc. If three of these have been correctly characterize above, then the other three would involve out-of-phase motion of th two types of magnesium atom, giving rise to weak absorption. It seem probable, too, that these vibrations would tend to couple only with th 'inactive' vibrations of the silicon-oxygen sheets, in which alternat oxygens of the inner layer (fig. 4) are 180° out of phase.

Finally, it may be noted that the rocking frequency of the structura hydroxyl groups has not been identified, nor have the bands which shoul arise from vibrations of the hydroxyl groups as a whole, out of phas with the other oxygen atoms of the inner layer in which they lie (fig. 4) These must be low-frequency vibrations, and in general it may be con cluded that whilst the identification of the origin of the higher-frequenc bands is probably satisfactory, the assignments in the low-frequenc region must be regarded as tentative. It would be desirable to extend the spectra to lower frequencies and also to study a talc in whic deuterium has been substituted for hydrogen.

Saponite and hectorite. The structures of saponite and hectorite ar derived from that of talc by isomorphous substitution: in saponite th substitution is mainly aluminium for silicon, while in hectorite substitu tion of lithium for magnesium and fluorine for hydroxyl occurs. In bot minerals the result is to give the layers of the clay minerals a negativ charge, which is compensated by exchangeable cations that lie betwee the layers. With the exchangeable cations is associated a water laye of variable thickness, which gives the characteristic swelling propertie

of these smectites. Corresponding to their structural similarities, the analogy between the spectra of talc and saponite is close, and the hectorite spectrum is clearly related, so that there is no difficulty in correlating the principal features of their spectra, as has been done in table I.

The shape and position of the magnesium silicate absorption bands of the smectites is insensitive to changes in either the water content or the exchangeable ions, so that the broadening of their bands compared with those of talc must be due principally to the damping effect of isomorphous substitution within the layers. That the broadening is more pronounced in hectorite can perhaps be correlated with the great change in valency and mass when lithium is substituted for magnesium. The change is proportionally less in both respects when aluminium is substituted for silicon, as in saponite.

It may be noted that it is the symmetrical distribution of magnesium ions with respect to the silicon-oxygen tetrahedra that largely preserves the hexagonal symmetry of the silicon-oxygen framework in talc. In its aluminium analogue, pyrophyllite, there are aluminium ions in only two of the three positions occupied by magnesium in talc. Because of the lower effective symmetry, pyrophyllite has a more complex spectrum (Beutelspacher, 1956*b*), in which none of the absorption bands in the region 650 to 1100 cm.$^{-1}$ appear, from the spectra of oriented films, to be polarized perpendicularly to the silicate sheets. In hectorite the replacement of some of the magnesium atoms of talc by lithium must disturb the vibrations of the silicate sheet in a similar but less regular manner, and it may be for this reason that its perpendicularly polarized bands are poorly defined. In saponite the aluminium-for-silicon substitution lies on threefold axes, and so has a more symmetrical effect on the surrounding structure. This agrees with its well-defined perpendicular bands.

The general broadening of the bands resulting from isomorphous substitution in talc is readily understood. In the infra-red- and Raman-active vibrations of a homogeneous crystal, the unit cells over a considerable area are in phase. Indeed, in talc the individual tetrahedra of a silicon-oxygen layer are either in phase or else alternate tetrahedra are 180° out of phase. The presence of a foreign atom in some of the tetrahedra, for example, will distort both the structure of neighbouring tetrahedra and also the form and natural frequency of their vibrations through shared oxygen atoms. In saponite, where the substitution is one in eight (Mackenzie, 1957), nearly half the silicon tetrahedra have an

aluminium-containing tetrahedron as a first neighbour. In consequence the sharp absorption band of talc is replaced by a broader band corresponding to the coupling of out-of-resonance vibrations. Even as it is no longer possible for the tetrahedra to be in phase, similarly it becomes impossible for them exactly to cancel each other. As a consequence the inactive vibrations of talc can become active, and in saponite and hectorite this may account for some of the weaker bands that are found in their spectra.

Absorption bands of the structural hydroxyl groups and of interlayer water.

The stretching frequencies of the structural hydroxyl groups in talc saponite, and hectorite all give rise to weak sharp bands at 3670 cm.$^{-1}$ which is 20 cm.$^{-1}$ lower than the corresponding band of brucite. These bands are very much weaker than the corresponding absorption bands of the dioctahedral minerals, pyrophyllite and montmorillonite. Saponite has an additional weaker sharp band at 3697 cm.$^{-1}$, and so resembles the magnesium mica, phlogopite, which also has doublet absorption at these frequencies. The higher-frequency component of the mica doublet is, however, the stronger. Hectorite, too, has an additional weaker but broader band at 3610 cm.$^{-1}$, which was detectable only after removing most of the interlayer water. In this it resembles the mica biotite which absorbs at 3670 and 3600 cm.$^{-1}$. In talc and saponite the hydroxyl groups are linked only to three magnesiums, and in hectorite the majority are also so linked, although there lithium is substituted for some of the magnesiums. The appearance of an absorption band common to all three minerals is therefore easily understood, but further work is necessary to identify the origin of the additional bands of the smectites.

Whilst talc has a broad weak band due to the stretching modes of adsorbed water at 3413 cm.$^{-1}$, the smectites show strong absorption in this region arising mainly from interlayer water. The broad diffuse bands consist of at least three components, as can be particularly clearly seen in the spectrum of sodium-saturated saponite (fig. 6A). In calcium and magnesium-saturated saponite, the outlying absorption bands are little affected in position and intensity, but the central peak increases and shifts to lower frequencies (table II). In caesium-saturated saponite all three absorption bands are weak at room temperature (fig. 6B). That these bands are due to interlayer water is established by their disappearance from a spectrum of caesium-saturated saponite, recorded after heating a pressed disk containing the saponite to 80° C. for 16 hours

(fig. 6c). The water-absorption bands of calcium-saturated hectorite are identical with those of the corresponding saponite, but in calcium-saturated montmorillonite the absorption band of the structural hydroxyl group, at 3630 cm.$^{-1}$, overlies the highest-frequency water-absorption band. There is little doubt, however, that this water absorption is also present in montmorillonites, leading to marked changes with water content in the apparent intensity of the structural hydroxyl absorption, which is always an outstanding feature of montmorillonite spectra in this region (Beutelspacher, 1956 *a*, *b*; Buswell and Dudenbostel, 1941). In contrast, the structural hydroxyl group absorption of trioctahedral minerals can scarcely be resolved from the adjacent water absorption at room humidity. Similar three-banded water absorption is found in vermiculite, whose interlayer-water structure is probably very similar to that of smectites.

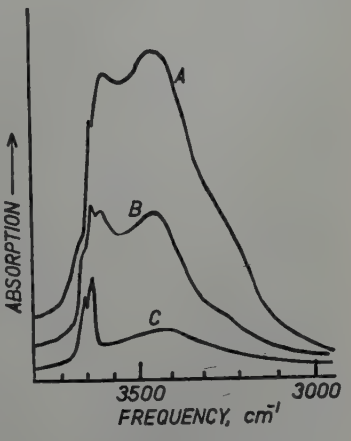

FIG. 6. Absorption of saponite (1·6 mg./cm.^{2} in pressed disks) due to the O–H stretching vibrations of the structural hydroxyl group and of interlayer water. A, Na^+-saturated; B, Cs^+-saturated; C, Cs^+-saturated, dried 16 hours at 80° C.

One type of water molecule can give rise to at most two O–H stretching frequencies. More commonly, adsorbed water such as is found in pressed alkali-halide disks, gives only one asymmetric band. Accordingly,

TABLE II. Frequencies (cm.$^{-1}$) of O–H stretching frequencies of interlayer water in saponite.

Exchangeable ion.			
Mg^{++}	Ca^{++}	Na^+	Cs^+
3610	3610	3620	3630
3400	3420	3440	3460
3260	3260	3260	3250

we must postulate at least two types of water molecule in these smectites. Using the empirical relationship derived by Glemser and Hartet (1955), we find that the higher-frequency absorption near 3620 cm.$^{-1}$ corresponds to a weak hydrogen bond with an H_2O–O distance exceeding 3 Å, The central maximum corresponds to an H_2O–O distance increasing from 2·75 Å. in Mg^{++}-saturated saponite to 2·85 Å. in Cs^+-saturated saponite,

and the low-frequency shoulder to an H_2O–O distance of 2·63 Å. The empirical relationship, however, applies strictly only when crystal water is bonded to an oxygen atom of an oxy-anion, and is not wholly applicable to saponite, where bonds between water molecules will also occur. Nevertheless, the evidence for three very different types of hydrogen bonding is strong. Mathieson and Walker (1954; see also Walker, 1956) have derived a detailed picture of the interlayer-water structure of a vermiculite phase with a 001 spacing of 14·36 Å., from which it is concluded that in the vicinity of a cation site the water molecules are coordinated around the magnesium atoms in an octahedron, in which each water molecule forms a strong hydrogen bond with a neighbouring oxygen of the silicate sheet (H_2O–O distance 2·90 Å.), and a very weak bond with adjacent water molecules. The presence of such a weak bond is in agreement with the infra-red measurement, but Mathieson and Walker's structure does not include a short enough hydrogen bond to account for the lowest-frequency absorption band at 3260 cm.$^{-1}$. A detailed comparison of infra-red measurements with the postulated structure must, however, be based on more closely controlled humidity conditions than has been possible here, and a better understanding of the infra-red absorption of water molecules in crystalline hydrates and in the adsorbed state.

In addition to the stretching vibrations discussed above, and to the broad H–O–H angle deformation frequency at 1640 cm.$^{-1}$, the interlayer water was found to give rise to diffuse unspecific absorption throughout the 900 to 600 cm.$^{-1}$ region, corresponding to the hindered rotation found in liquid water at 710 cm.$^{-1}$ (Giguere and Harvey, 1956). The corresponding band in crystalline hydrates can move up to 800 cm.$^{-1}$, where it now represents a rocking of water molecules coordinated round cations.

Effects of grinding on the infra-red spectra of layer minerals.

As previously noted, grinding these layer minerals in the vibratory-ball mill caused marked changes in their spectra, which occurred most rapidly when small quantities were ground. Changes in infra-red spectra, and in other physical and chemical properties of clays (Perkin *et al.*, 1955) and micas (Mackenzie, Meldau, and Farmer, 1956) have been noted after grinding in an agate mortar or rotary ball-mill for periods varying from 8 hours to 6 weeks: these changes indicate the formation of an amorphous product. It is clear, however, from arguments used in discussing the broadening due to isomorphous substitution, that very

small particle size must also lead to broadening of the absorption bands, due to the effects of the disrupted structure at the particle edges, but it is not clear at what particle size it will first produce striking changes in the spectra. It may be, however, that this stage is reached when talc is

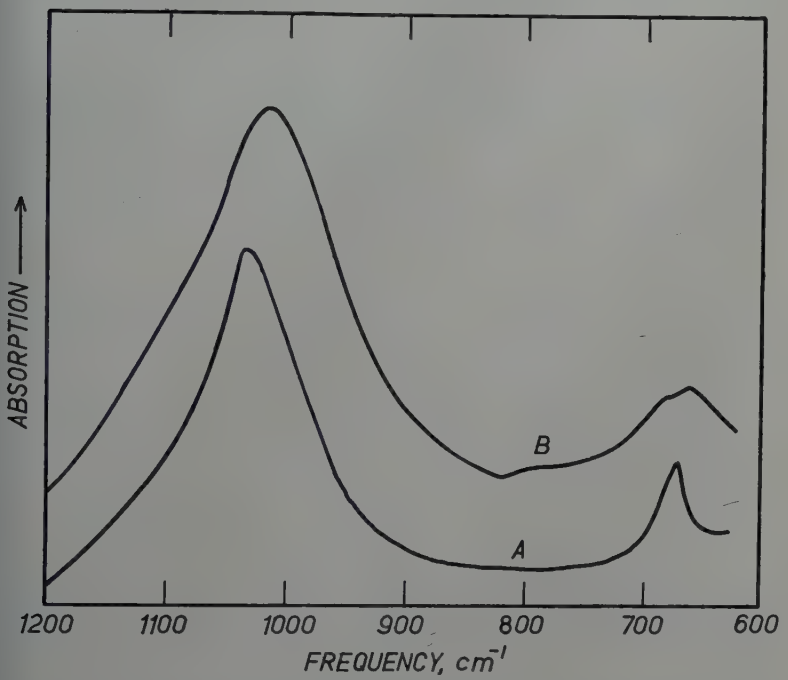

FIG. 7. Effect of grinding on the infra-red absorption of talc (A) and saponite (B). The spectra were obtained from pressed disks, 15 mg. of the minerals having been previously ground alone for 10 minutes in the vibratory grinder.

ground in the vibratory ball-mill (fig. 7). The persistence of the absorption band at 670 cm.$^{-1}$ indicates that the talc structure persists to some degree, since this absorption band does not occur in amorphous silica or magnesium oxide. Unlike the Si–O vibrations, the O–H stretching vibrations should not be greatly affected by particle size, since coupling between adjacent hydroxyl groups can only be weak. This absorption does, in fact, remain sharp and well defined after the Si–O vibrations have markedly broadened. The spectral changes are therefore consistent with a small particle size, or with numerous dislocations in the structure of larger particles, perpendicular to the plane of the sheets. Separation

of the mineral into individual sheets should have little effect on the spectra, since mechanical coupling between vibrations in different sheets is slight.

Grinding of saponite under similar conditions also leads to a broadening of its Si–O absorption bands. In addition, a broad diffuse band appears near 1430 cm.$^{-1}$, which probably arises from carbonate formation, and so indicates some breakdown in the saponite structure.

Acknowledgements. I am grateful to Dr. R. C. Mackenzie for the specimens of the minerals examined, and for his helpful interest and encouragement during this work. I am indebted to Dr. D. C. McKean, Chemistry Department, University of Aberdeen, for a very helpful discussion of the assignments, and for infra-red measurements in the region 650 to 400 cm.$^{-1}$, also to Mr. W. A. Mitchell and Miss W. W. Smith for estimating the orientation of clay deposits by X-ray diffraction.

References.

Adler (H. H.), Kerr (P. F.), Bray (E. E.), Stephens (N. P.), Hunt (J. M.), Keller (W. D.), and Pickett (E. E.), 1951. Infrared spectra of reference clay minerals, Amer. Petroleum Inst., Res. Proj. 49.

Ardenne (Manfred von), 1941. Angew. Chem., vol. 54, p. 144.

Beutelspacher (H.), 1956*a*. 6th International Congress of Soil Science. Reports, vol. B (Commissions 1 and 2), p. 329.

—— 1956*b*. Landw. Forsch., Sonderheft No. 7, p. 74.

Bragg (W. L.), 1937. Atomic Structure of Minerals. New York, Cornell Univ. Press.

Buswell (A. M.) and Dudenbostel (B. F.), 1941. Journ. Amer. Chem. Soc., vol. 63, p. 2554.

Downie (A. R.), Magoon (M. C.), Purcell (T.), and Crawford (B., *Jr.*), 1953. Journ. Opt. Soc. Amer., vol. 43, p. 941.

Duval (C.) and Lecomte (J.), 1954. Compt. Rend. Acad. Sci. Paris, vol. 239, p. 249.

Farmer (V. C.), 1956. Spectrochimica Acta, vol. 8, p. 374.

Ford (M. A.), Wilkinson (G. R.), and Price (W. C.), 1954. Molecular Spectroscopy (Edit. G. Sell). Inst. Petroleum, London, 1955; p. 82.

Giguere (P. A.) and Harvey (K. B.), 1956. Canad. Journ. Chem., vol. 34, p. 798.

Glemser (O.) and Hartet (E.), 1955. Naturwiss, vol. 42, p. 534.

Hertzberg (G.), 1945. Infrared and Raman Spectra of Polyatomic Molecules. New York, D. van Nostrand Co., Inc.

Hexter (R. M.) and Dows (D. A.), 1956. Journ. Chem. Physics, vol. 25, p. 504.

Hunt (J. M.), Wisherd (M. P.), and Bonham (L. C.), 1950. Anal. Chem., vol. 22, p. 1478.

—— and Turner (D. S.), 1953. Anal. Chem., vol. 25, p. 1169.

Launer (P. J.), 1952. Amer. Min., vol. 37, p. 764.

Lax (M.) and Burstein (E.), 1955. Phys. Rev., vol. 97, p. 39.

Mackenzie (R. C.), 1957. Min. Mag., vol. 31, p. 672.

—— Meldau (R.), and Farmer (V. C.), 1956. Ber. deut. keram. Ges., vol. 33, p. 222.

Mathieson (A. McL.) and Walker (G. F.), 1954. Amer. Min., vol. 39, p. 231.

Mathieu (J.-P.), 1945. Spectres de Vibration et Symetrie des Molecules et des Cristaux. Paris, Herman et Cie.

Matossi (F.) and Bronder (O.), 1938. Zeits. Physik, vol. 111, p. 1.

Nahin (P. G.), 1955. Clays and Clay Technology. Bull. 169, Dept. Nat. Resources, Div. Mines, California, p. 112.

—— Merrill (W. C.), Grenall (A.), and Crog (R. S.), 1951. Journ. Petrol. Tech., vol. 3, p. 151.

Perkins (A. T.), Dragsdorf (R. D.), Lippincott (E. R.), Selby (J.), and Fateley (W. G.), 1955. Soil Sci., vol. 80, p. 109.

Roy (D. M.) and Roy (R.), 1957. Geochimica Acta, vol. 11, p. 72.

Walker (G. F.), 1956. Clays and Clay Minerals (Edit. A. Swineford), Publ. 456, Nat. Acad. Sci., Nat. Research Council, Washington, D.C.

Weiler (J.), 1932. Nature, vol. 130, p. 893.

The mineral paragenesis and metamorphic status of garnet–hornblende–pyroxene–scapolite gneiss from Ghana (Gold Coast).

By O. von Knorring, Ph.D., and W. Q. Kennedy, D.Sc., F.R.S.

Dept. of Geology, University of Leeds.

[Read 27 March 1958.]

Summary. The main minerals (garnet, pyroxene, hornblende, and scapolite) in certain Dahomeyan (Archaean) garnet–hornblende–pyroxene–scapolite gneisses from Ghana have been separated and analysed. Both the garnet and the pyroxene show marked eclogitic affinities, and the rocks are considered to occupy a transitional position between the amphibolite and eclogite facies. The scapolite is a sulphatic variety containing more than 4 % SO_3 and is believed to be a product of autometasomatism. A revised scheme for the distribution of mineral facies within the temperature-pressure field of metamorphism is proposed.

Part I. Paragenetical mineralogy.

By O. von Knorring.

THE rocks with which the present paper deals belong to a great belt of basic Archaean (Dahomeyan) gneisses, from 2 miles up to 15 miles or so in width, that extends across the south-eastern corner of Ghana, from the coast-line east of Accra, through the area of the Shai Hills, and across the Volta River into the adjacent territory of Togoland (see map, fig. 1). This belt consists predominantly of very uniform, coarse, sometimes massive, but usually well-foliated garnetiferous hornblende gneisses and granulites with distinctive pale-coloured felspathic bands (Junner and Bates, 1945, pp. 1–23), but also includes, according to Junner (op. cit., p. 7), pyroxene-gneisses and eclogites, at least in the coastal section to the south.

The rocks have not yet been studied in detail and little is known concerning the variety and distribution of petrographical types. It has now been recognized, however, as a result of our own recent investigations, that pyroxene- and scapolite-bearing varieties are rather well developed in the area of the Shai Hills, particularly in the inselberg Mampong at the south-eastern extremity of the region, and may, in view of the uniform character of the metamorphism, eventually prove

to have a much wider regional distribution. These types are of considerable interest, moreover, in that they contain a sulphate-rich carbonate-scapolite in stable paragenetical association with a suite of minerals including typical members of both the amphibolite and eclogite facies. A rather detailed mineralogical and mineral-chemical study has therefore

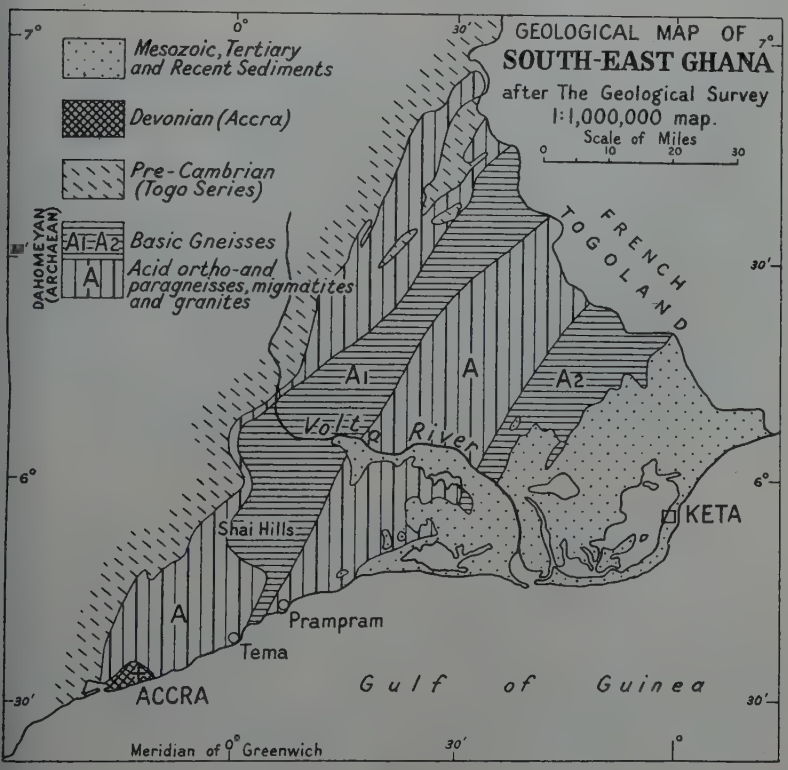

Fig. 1.

been carried out in order to assess the possible significance of the paragenesis in relation to the general scheme of metamorphic facies classification.

Character of the rocks.

The pyroxene- and scapolite-bearing rocks of the Shai Hills are mineralogical variants of the common garnetiferous hornblende gneisses from which they cannot readily be distinguished in hand specimens. Whereas pyroxene is widely distributed and must be regarded as a

normal constituent of the Dahomeyan garnetiferous hornblende gneisses, it would appear that scapolite is probably restricted in its occurrence, and may be confined to definite horizons and specific areas. The most typical scapolite-bearing rocks so far identified are those from the inselberg Mampong, at the south-eastern extremity of the Shai Hills, but insufficient work has been carried out to justify any definite statement about the regional distribution of the mineral.

As in the case of the normal garnetiferous hornblende gneisses, the scapolite-bearing rocks are usually highly foliated and present a characteristic streaky or finely striped appearance due to the lenticular or rodded development of the various constituents. Garnets are abundant, both as tiny crystals scattered throughout the body of the rock and as larger porphyroblasts, which in extreme cases may attain a diameter of several inches. Normal gneissic banding is not developed, but small-scale compositional banding due to the segregation of garnet-rich and pyroxene-rich layers is sometimes seen, as in the analysed scapolite-rich rock from Mampong. Light-coloured felspathic bands are developed locally and may in individual cases attain a thickness of a foot or more. In addition, tiny veinlets of oligoclase, containing megascopically visible scapolite, occasionally intersect the foliation of the rocks.

Under the microscope the rocks are seen to consist of a coarsely granoblastic aggregate of garnet, hornblende, pyroxene, scapolite, oligoclase, and quartz as major constituents, together with accessory rutile and apatite, a little magnetite and ilmenite, and some secondary epidote and calcite (fig. 2). The *garnet* is pinkish in colour and is usually xenoblastic in habit. Rarely, idioblastic boundaries are developed against oligoclase. Inclusions of quartz and rutile are common, but kelyphitic rims and other evidences of reaction are conspicuously lacking. Certain of the garnets from the Mampong area show a rather unusual type of orientated intergrowth in which extremely fine rods of some anisotropic mineral are arranged in a triangular pattern similar to the exsolution intergrowth of ilmenite in magnetite (fig. 3); the identity of the intergrown mineral has not yet been established. The *clinopyroxene* is a pale greenish non-pleochroic variety which in its general appearance is similar to diopside-hedenbergite. It may also contain inclusions of quartz and magnetite and, in certain cases, shows incipient uralitization. *Hornblende* is the predominant dark mineral and the most prominent constituent of the rocks. It shows a straw-yellow–dark-green–brownish-green pleochroism, but is not distinguished by any special peculiarities in

thin section. On the other hand, the *scapolite* instantly attracts attention by its high refringence and birefringence and by its local abundance. The mineral occurs throughout the body of the rocks and, in addition, is often concentrated in veinlets and bands. In its present setting the scapolite is not an alteration product of plagioclase or any other mineral but is a stable primary constituent of the rock, in full equilibrium with

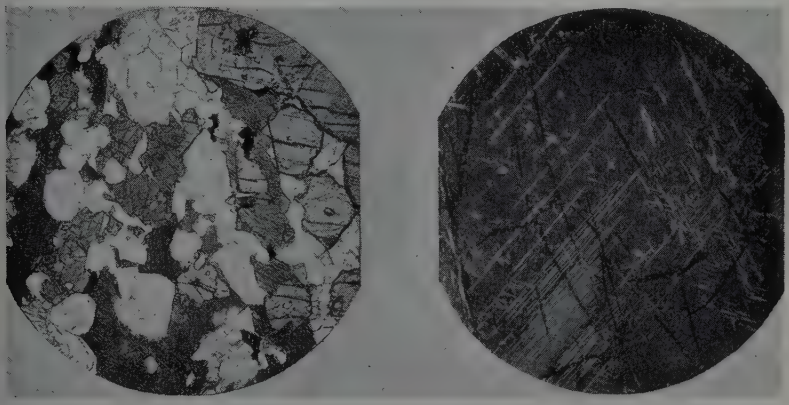

Fig. 2. Fig. 3.

Fig. 2 (*left*). A scapolite-rich variety of the garnet–pyroxene–hornblende-scapolite gneiss. Most of the white mineral is scapolite. ×15.

Fig. 3 (*right*). Lamellar and rod-like intergrowth in garnet. Crossed nicols. ×28.

the accompanying minerals. It is significant in this connexion that porphyroblasts of scapolite are occasionally developed in a matrix of quartz and oligoclase. *Rutile* is typomorphic and is present in the form of dark brown, irregular, elongated, and boomerang-shaped grains. Its occurrence is particularly significant as rutile is generally regarded as a characteristic constituent of basic rocks belonging to the eclogite and granulite facies.

Two of the scapolite-bearing gneisses have been analysed and the results are set out in table I.

The rock from Mampong (anal. 1) represents a basic segregation band with approximately 20 % of scapolite: that from the 'Shai Hills' (anal. 2) may be taken as fairly representative of the formation as a whole and is an otherwise normal garnet–hornblende–pyroxene gneiss, but contains approximately 2 % of scapolite.

The original basic igneous character of the rocks is clearly indicated by these analyses, which are comparable with those of certain gabbros

TABLE I

	1.	2.	3.	4.	Norm. of 1.	Norm. of 2.
SiO_2	42·12	50·00	43·32	49·68	or 1·7	or 1·7
TiO_2	0·89	1·00	0·80	0·23	ab 13·6	ab 37·8
Al_2O_3	18·95	19·53	18·22	20·86	an 38·4	an 32·5
Fe_2O_3	4·36	2·85	5·84	1·02	ne 5·4	di 8·1
FeO	9·50	5·55	6·26	5·52	di 10·5	hy 0·2
MnO	0·20	0·07	0·09	—	ol 19·5	ol 11·6
MgO	7·63	5·59	8·42	6·50	mt 6·3	mt 4·2
CaO	11·26	9·28	11·48	10·77	il 1·7	il 1·9
Na_2O	2·76	4·48	2·34	3·46	ap 0·3	ap 0·7
K_2O	0·28	0·32	0·18	1·38	cc 1·4	cc 0·5
H_2O+	0·84	0·64	1·91	0·53	$\frac{sal}{fem} = 1·5$	$\frac{sal}{fem} = 2·7$
H_2O-	0·02	0·00	0·28	—		
P_2O_5	0·09	0·32	0·09	0·00		
CO_2	0·60	0·20	0·19	—		
SO_3	0·86	0·09	—	0·26†		
Total	100·36	99·92	99·42	100·21		

† S.

1. Garnet–hornblende–pyroxene–scapolite gneiss from Mampong, Ghana. Anal. M. H. Kerr. F and Cl, tr.
2. Garnet–hornblende–pyroxene–scapolite gneiss from Shai Hills, Ghana. Anal. M. H. Kerr. F and Cl, tr.
3. Kyanite–eclogite from Roberts-Victor mine, Kimberley. Anal. J. Parry. (Analyses of rocks and minerals, Geol. Surv. Mem., no. 32, p. 187, Union of South Africa, 1938.)
4. Garnet–pyroxene–labradorite from Sebo, Norway (Eskola, 1921, p. 92).

and basalts, and more particularly with eclogite rocks from various localities (Eskola, 1921, p. 92; Alderman, 1936, p. 488). The petrographical uniformity of the formation and the complete absence of relict sedimentary banding are also indicative of an original igneous character, but, as the rocks have been entirely reconstituted under conditions of deep-seated metamorphism, and have lost all trace of original structures, it is impossible to specify whether they were of volcanic or intrusive origin.

Mineral chemistry.

The main mineral constituents (garnet, pyroxene, hornblende, and scapolite) in the gneiss from Mampong (anal. 1, table I) were separated by means of Clerici solution and a magnetic separator, and pure samples for analysis were finally prepared by hand-picking under a binocular microscope. The analyses, together with the optical data, are shown in tables II–IV, below.

The analysed minerals all show peculiarities of composition that are

TABLE II. Chemical composition of garnets from the Mampong gneiss compared with those of garnets from some eclogites.

	1.	2.	3.	4.	5.
SiO_2	39·50	38·73	39·76	40·3	40·30
TiO_2	0·16	0·34	—	tr.	tr.
Al_2O_3	21·53	19·76	22·04	21·6	21·86
Cr_2O_3	tr.	—	—	—	—
Fe_2O_3	1·05	5·45	1·37	1·3	2·16
FeO	20·91	19·31	18·06	18·0	19·08
MnO	0·66	—	—	0·7	0·69
MgO	7·85	8·92	8·92	11·2	11·28
CaO	8·34	7·87	10·42	7·2	5·22
Total	100.00	100·38	100·57	100·3	100·59
Sp. Gr.	3·93	—	—	3·74	3·88
n	1·773±0·002	—	—	1·756	1·766
a, Å.	11·59±0·05	—	—	—	—

Atomic ratios to 96 oxygen, anal. 1: $Mg_{7\cdot2}Fe^{2+}_{10\cdot7}Mn_{0\cdot3}Ca_{5\cdot5}Al_{15\cdot5}Fe^{3+}_{0\cdot5}Si_{24\cdot1}O_{96}$.

1. Garnet from garnet–pyroxene–hornblende–scapolite gneiss, Mampong, Ghana. Anal. O. von Knorring.
2. Garnet from eclogite, Schutthalde, Tyrol (Alderman, 1936, p. 499).
3. Garnet from eclogite, Saint-Philbert de Grandlieu (Alderman, 1936, p. 499).
4. Garnet from eclogite, Beinn à Chapuill, Glenelg (Alderman, 1936, p. 498).
5. Garnet from eclogite, Silden, Norway (Eskola, 1921, p. 38).

highly significant in relation to the metamorphic status and character of the rocks.

In the first place, the composition of the *garnet* (table II) is unusual in that both Mg and Ca are relatively high, indicating a lime-bearing pyrope-almandine with some 26 % of pyrope and approximately 20 % of grossular. Garnets of this type, in which there has been appreciable substitution of Fe by Mg and Ca, are not formed under the normal metamorphic conditions of the amphibolite facies, but are, on the other hand, typically developed in eclogites, granulites, and related high pressure rocks.

The composition of the *clinopyroxene* (table III) is also indicative of high-pressure conditions as the Al_2O_3 and Na_2O content is that of an omphacitic variety of diopside-hedenbergite with approximately 10 % of jadeite component. The jadeite component is admittedly considerably lower than in true omphacites, but the mineral is nevertheless clearly related in composition to the eclogitic pyroxenes.

A similar tendency is perhaps also apparent in the case of the *hornblende* (table IV) which compares closely in composition with hornblendes from garnet–amphibolites of eclogitic derivation. Hastingsitic amphiboles of this type are, however, more widely distributed and are consequently less significant in regard to metamorphic facies.

TABLE III. Chemical composition of pyroxene from the Mampong gneiss compared with those of pyroxenes from some eclogites.

	1.	2.	3.	4.
SiO_2	49·60	48·11	55·56	53·48
TiO_2	0·62	0·97	0·15	1·04
Al_2O_3	6·12	7·55	7·17	9·52
Fe_2O_3	3·80	8·18	2·82	3·00
FeO	5·86	5·38	2·06	5·84
MnO	0·10	—	0·05	—
MgO	11·26	12·97	11·32	6·34
CaO	20·58	15·10	16·85	14·87
Na_2O	1·68	1·60	3·92	3·97
K_2O	0·05	0·30	0·57	0·63
H_2O+	0·25	—	0·08	0·73
H_2O-	0·05	—	—	—
Total	99·97	100·16	100·55	99·42
Sp. Gr.	3·35	—	3·33	3·31
α	1·689	—	—	—
β	1·699	—	1·683	1·700
γ	1·718	—	—	—
$2V_\gamma$	64°	—	67°	—

Atomic ratios to 48 oxygen (anal. 1): $C_{6.6}Na_{1.0}Mg_{5.0}Fe^{2}_{1.5}(Fe^{3}+Ti,Al)_{2.0}Al_{1.2}Si_{14.8}O_{48}$

1. Pyroxene from garnet–pyroxene–hornblende-scapolite gneiss, Mampong Gold Coast (Ghana). Anal. O. von Knorring.
2. Pyroxene from labradorite rock Alvaerstrømmen, Norway (Eskola, 1921 pp. 91–92).
3. Pyroxene from eclogite, Silden, Norway (Eskola, 1921, p. 38).
4. Pyroxene from eclogite, Glenelg (Alderman, 1936, p. 494).

Finally, the *scapolite* (table IV) is particularly interesting in that the content of SO_3 is higher than in any scapolite so far analysed. At the same time, Cl is virtually absent although the majority of rock-forming scapolites are Cl- and CO_2-bearing varieties. Few complete analyses are available for comparison, but the mineral is seen to compare most closely with scapolites in ejectamenta from the Laacher See and in skarn rocks from Laurinkari in Finland. It may be emphasized that the scapolite from the Shai Hills is not a secondary product replacing some existing mineral such as plagioclase but is a primary constituent of the paragenesis, and is in completely stable equilibrium with the associated minerals.

Discussion of results.

The chemical and mineralogical examination of the basic gneisses from the Shai Hills leads to the conclusion that the rocks must have formed under metamorphic conditions transitional between those of the

TABLE IV. Chemical composition of hornblende from the Mampong gneiss compared with those of some other hornblendes of eclogitic origin; and composition of scapolite from the Mampong gneiss compared with some other sulphatic scapolites.

	1.	2.	3.	4.	5.	6.	7.
SiO_2	41·86	42·17	46·68	42·28	47·52	46·25	46·59
TiO_2	1·90	1·00	0·35	0·66	none	—	—
Al_2O_3	14·31	13·46	14·37	17·24	25·21	26·50	26·33
Fe_2O_3	4·29	5·92	4·00	2·68	—	—	—
FeO	8·79	7·82	8·29	9·34	0·30	0·13	1·31
MnO	0·10	0·15	—	0·12	0·02	—	—
MgO	12·58	14·46	11·71	11·91	0·14	0·17	0·52
CaO	11·14	11·76	10·32	11·06	15·48	16·03	15·70
Na_2O	2·47	0·68	2·41	1·73	4·52	3·96	3·68
K_2O	0·63	0·80	0·54	0·81	0·10	0·57	1·11
H_2O+	1·84	1·53	1·06	2·05	0·22	1·16	0·80
H_2O-	0·08	—	0·23	0·08	0·08	—	—
P_2O_5	—	—	—	—	0·03	—	—
CO_2	—	—	—	—	2·16	3·12	3·52
F	n.d.	—	—	—	none	—	—
Cl	0·07	—	—	—	0·06	0·72	tr.
SO_3	—	—	—	—	4·17	1·41	2·06
Total	100·06	99·75	99·96	99·96	100·01	100·02	101·62
Sp. gr.	3·22	3·13	—	3·20	2·72	2·71	2·75
α	1·659±0·001	—	—	1·648	ω 1·587±0·001	1·580	1·5872
β	1·673±0·001	1·65	—	—	ϵ 1·564±0·001	1·553	1·5595
γ	1·678±0·001	—	—	1·672			
$2V_\alpha$	75°	—	—	84°			
$c:\gamma$	13°	26°	—	19°			

Atomic ratios to 48 (O,OH) (anal. 1):

$$(Na,K)_{1\cdot6}Ca_{3\cdot5}Mg_{5\cdot5}Fe^{2+}_{2\cdot1}(Al,Fe^{3+},Ti)_{2\cdot5}(OH)_{4\cdot0}(Si,Al)_{16}O_{44}.$$

1. Hornblende from garnet–pyroxene–hornblende–scapolite gneiss, Mampong, Ghana. Anal. O. von Knorring.
2. Hornblende from garnet–amphibolite, Beinn à Chapuill, Glenelg (Alderman, 1936, p. 519).
3. Hornblende from Umhausen (Alderman, 1936, p. 520).
4. Hornblende from kyanite–garnet–amphibolite, Glenelg (Tilley, 1937, p. 566).
5. Scapolite from garnet–pyroxene–hornblende–scapolite gneiss, Mampong, Ghana. Anal. O. von Knorring.
6. Scapolite from Laurinkari, Finland (Borgström, 1913).
7. Scapolite from Laacher See (Niggli, 1926).

amphibolite and eclogite facies. This is seen in the association of the typical amphibolite minerals, hornblende and plagioclase, with garnets and pyroxenes of distinctive eclogitic type. A somewhat similar paragenesis, in which, however, hornblende and plagioclase are associated with *normal* types of almandine and diopside, has been recognized by Korzhinsky (Korzhinsky, 1937, p. 393), and is referred by Turner (Turner and Verhoogen, 1951, p. 458) to an almandine–diopside–horn-

blende subfacies, which he regards as transitional between the amphi bolite and granulite facies. In view of the marked differences in th chemistry of the equivalent minerals it is not possible, however, to assig the rocks of the Shai Hills to this subfacies, and they are consequentl regarded as possessing a different status in metamorphism.

It is proposed, therefore, to recognize two mineralogically simila amphibolite parageneses, characterized by the association garnet- pyroxene–hornblende, and represented by the almandine–diopside hornblende subfacies on the one hand, and the gneisses of the Sha Hills on the other. These are considered to be transitional to the granul ite and eclogite facies respectively, and are distinguishable only on th basis of mineral chemistry. In both instances, moreover, affinities wit the higher metamorphic facies are emphasized by the presence of rutil as a characteristic accessory mineral.

Amphibolitized eclogites, possessing mineralogical characters simila to those of the Shai Hills gneisses, are by no means uncommon as pro ducts of retrograde metamorphism, but differ fundamentally in origi from the rocks in question, which are progressive types that have jus failed to attain the full status of eclogites.

The presence of scapolite in certain of the gneisses also present features of considerable interest as the mineral has not formed throug any contact action but appears to be a normal product of the mai regional metamorphism. This is important in view of the fact tha scapolitization is generally regarded as an essentially metasomatic pro cess associated with the introduction of fugitive constituents such a H_2O, CO_2, Cl, and SO_3. So far as chlorine is concerned, an externa source must usually be postulated, and Buddington (1939, p. 267), fo example, attributes the formation of the chlorine-bearing scapolite in th metagabbros and basic gneisses of the north-western Adirondacks t metamorphic processes connected with the intrusion of granite magmas In the Cloncurry district of north-western Queensland, moreover, th process has operated on a regional scale (Edwards and Baker, 195 pp. 1–33), and the widespread development of scapolite–diopsid granulites is there related to regional scapolitization connected with th albitization of calcareous shales. The source of the emanations is ur known, but the metasomatism appears to have been contemporaneou with regional metamorphism, and the scapolite is predominantly Cl-bearing dipyre.

An extraneous source for the fugitive constituents is not alway necessary, however, and, in particular, CO_2- and SO_3-bearing scapolite

such as those from the Shai Hills, may well have formed through internal reactions of pre-existing minerals containing CO_2 and S (Ramberg, 1952, p. 268). This may apply also to certain scapolite-bearing amphibolites and pyroxene-gneisses from south-eastern Finland that have been described by Parras (1941, p. 493), and are considered to have originated under conditions of high-grade regional metamorphism allied to those of the granulite facies. The scapolite from this area has not been analysed, but on the basis of its optical properties it appears to be an almost pure meionite. It is interesting, therefore, that Sundius (1918, p. 104) has recognized two types of scapolite in the scapolite-amphibolites of Northern Sweden: soda-rich Cl-bearing scapolites formed through pneumatolytic action; and lime-rich CO_2-bearing scapolites formed during contact or deep-seated regional metamorphism *without* addition of extraneous fugitive constituents.

The scapolite of the Shai Hills falls within the second category and is considered to have formed through some process of autometasomatism involving the interaction of sulphide and other minerals present in the original rock. Geological observations indicate, moreover, that there is a rather constant occurrence of scapolite in association with eclogites and related rocks, and it is probable that the process of autometasomatism is dependent on the high temperatures and particularly on the high pressures involved.

There can be little doubt that the garnet–hornblende–pyroxene–scapolite gneisses of the Shai Hills represent original basic igneous rocks that have attained their present condition as a result of regional metamorphism under the influence of intense stress and high temperature. Assuming that the original rocks consisted mainly of olivine, pyroxene, and labradorite, as indicated by the norm, the following transformation process can be envisaged:

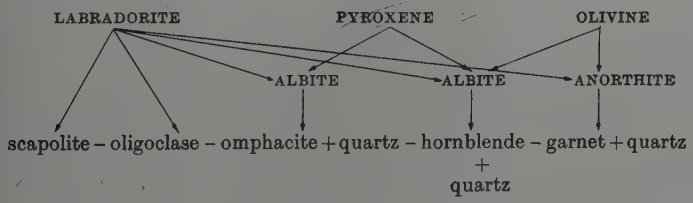

This is closely related to the 'eclogite reaction' and serves to emphasize the restricted stability of both albite and anorthite under the pressure–temperature conditions involved.

Part II. The distribution of mineral facies within the pressure–temperature field of metamorphism.

By W. Q. Kennedy.

The evidence provided by the foregoing detailed mineralogical an mineral-chemical study of garnet–hornblende–pyroxene–scapolite gneis from Ghana leads to certain interesting conclusions regarding the inte relationship of mineral facies within the pressure–temperature field c metamorphism.

It is the aim of facies petrology to subdivide the pressure–temperatu field of metamorphism in terms of the stability fields of individu mineral facies, and a *formalized* scheme, originally proposed by Esko (Eskola, 1920), and subsequently adopted by other writers (e.g. Turn and Verhoogen, 1951, p. 433) is shown below:

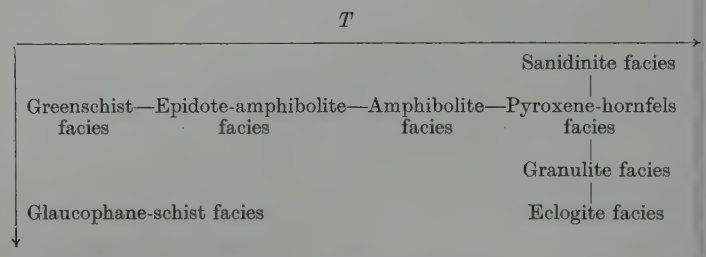

Each facies covers the stability range of a certain group of associate minerals, but within the general scheme there is variation in t stability fields of individual minerals or mineral components. T behaviour of the end components of the plagioclase felspar series, albi and anorthite, is particularly instructive in this connexion as it is possib to group the various facies on the basis of the stability, partial stabilit and instability of albite and anorthite respectively. Thus, in t granulite facies albite is stable, and albite-bearing plagioclases can exis In the eclogite facies, on the other hand, albite is completely unstab and is represented by the jadeite component of the pyroxene. Agai in the glaucophane-schists and in the garnet–hornblende–pyroxen scapolite gneiss from Ghana, a partial stability of albite can be reco nized as its constituents appear partly in the felspar and partly in t ferromagnesian mineral. Similarly, anorthite is stable in the granuli facies, where it appears in plagioclase felspar, but is completely unstab in the eclogite facies. The stability relationships of albite and anorthi in the various metamorphic facies are summarized in table V.

TABLE V. Stability relationships of albite and anorthite in metamorphic facies (+ indicates stable, − unstable, and +− partially stable).

Facies.		Albite.	Anorthite.
Greenschist		+	−
Epidote-amphibolite	Lower	+	−
	Upper	+	+−
Amphibolite		+	+
Pyroxene hornfels		+	+
Sanidinite		+	+
Granulite		+	+
Eclogite		−	−
Glaucophane schist		+−	−
Ghana gneiss		+−	+−

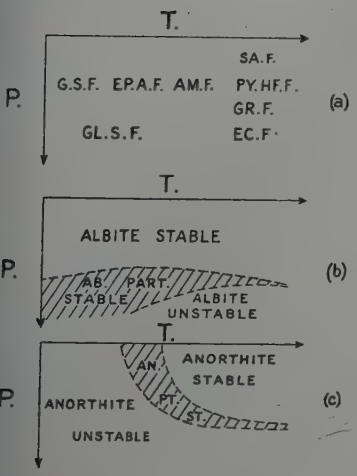

FIG. 4.

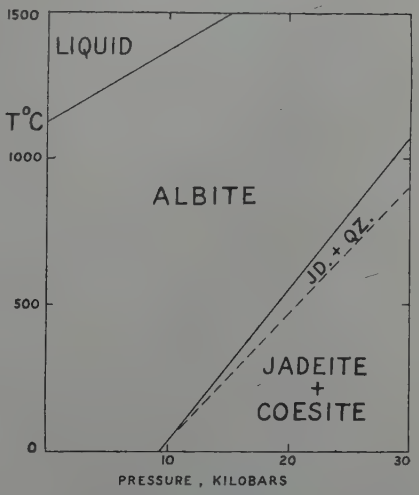

FIG. 5.

FIG. 4 (*left*). Stability fields of albite and anorthite in relation to metamorphic facies: (*a*) formalized scheme of facies distribution according to Eskola and others; SA.F. (Sanidinite facies), G.S.F. (greenschist facies), EP.A.F. (epidote-amphibolite facies), AM.F. (amphibolite facies), PY.HF.F. (pyroxene-hornfels facies), GR.F. (granulite facies), EC.F. (eclogite facies), GL.S.F. (glaucophane-schist facies); (*b*) and (*c*) stability fields of albite and anorthite plotted on basis of scheme (*a*).

FIG. 5 (*right*). Theoretical temperature–pressure relationships for the reaction albite = jadeite + quartz. According to Robertson, Birch, and MacDonald (1957).

It is possible to transfer these relationships to Eskola's formalized scheme of facies distribution and so to subdivide the pressure–temperature field of metamorphism on the basis of the stability behaviour of albite and anorthite; this is shown on fig. 4.

The most striking and significant feature is the very direct relation ship between pressure and the stability field of albite. Under th influence of pressure, albite is converted into jadeite plus quartz, th jadeite normally entering into the ferromagnesian mineral. Eskola' facies scheme is, however, a formalized one, but could be rendere

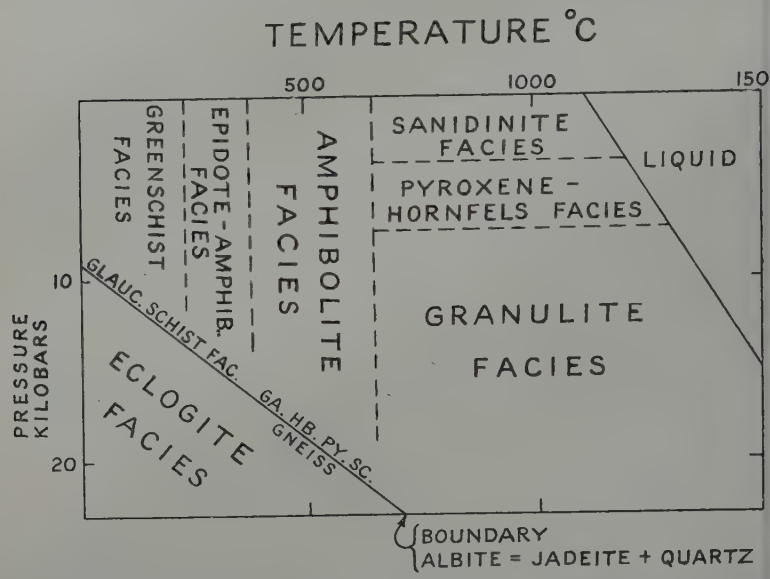

FIG. 6. Proposed scheme of facies distribution within the temperature-pressur field of metamorphism.

absolute on the basis of the stability relationships of albite and anorthit within the various facies, provided the pressure–temperature factors o the stability fields were known. No experimental data for anorthite ar available, but Robertson, Birch, and MacDonald (1957, p. 115) hav recently determined the stability relations of jadeite to 25 000 bars, an fig. 5 shows their theoretical temperature–pressure relations in the plan of (dry) albite compositions (op. cit., fig. 7, p. 132). This gives th position of the stability boundaries of albite against jadeite + quartz and can be utilized as a basis for a revised scheme of facies distributio within the pressure–temperature field of metamorphism. The revise scheme suggested by the present authors is shown in fig. 6.

This scheme is tentative and no validity is claimed for the tempera tures and pressures shown. It is believed, nevertheless, that the pro

posed facies distribution scheme does, in fact, provide a closer approximation to reality, and at least serves to explain some hitherto anomalous metamorphic rock associations and relationships.

Acknowledgements. The writers wish to express their indebtedness to Mr. W. G. Collins of Keir & Cawder Ltd. for assistance in the field, to Messrs. K. G. Cox and D. Abraham for the optical determinations on the analysed minerals, and to Mrs. M. H. Kerr for the rock analyses quoted in table I.

References.

Alderman (A. R.), 1936. Eclogites in the neighbourhood of Glenelg, Inverness-shire. Quart. Journ. Geol. Soc., vol. 92, p. 488.

Borgström (L. H.), 1913. Die Skapolithlagerstätte von Laurinkari. Bull. Comm. Géol. Finlande, No. 41.

Buddington (A. F.), 1939. Adirondack igneous rocks and their metamorphism. Geol. Soc. Amer., Mem. 7.

Edwards (A. B.) and Baker (G.), 1953. Scapolitization in the Cloncurry district of North-western Queensland. Journ. Geol. Soc. Australia, vol. 1, p. 1 [M.A. 12–421].

Eskola (P.), 1920. The mineral facies of rocks. Norsk. Geol. Tidsskr., vol. 6, p. 143.

—— 1921. On the eclogites of Norway. Skrifter Vidensk.-selskab. Kristiania. I. Mat.-Nat. Kl., no. 8 [M.A. 2–313].

Hall (A. L.), 1938. Analyses of rocks, minerals, ores, etc., from southern Africa. Dept. Mines, Geol. Surv. Mem. no. 32.

Junner (N. R.) and Bates (D. A.), 1945. Reports on the geology and hydrology of the coastal area east of the Akwapim range. Gold Coast Geol. Surv. Mem., no. 7.

[Korzhinsky (D. S.)] Коржинский (Д. С.), 1937. [Dependence of mineral stability on the depth.] Зап. Всеросс. Мин. Общ. (Mém. Soc. Russe Min.), vol. 66, no. 2, p. 369.

Niggli (P.), 1926. Lehrbuch der Mineralogie, vol. 2. Berlin, Borntraeger.

Parras (K.), 1941. Das Gebiet der Pyroxen führenden Gesteine im westlichen Uusimaa in Südfinnland. Geol. Rundschau (Suomi-Finnland Heft), Bd. 32, p. 484.

Ramberg (H.), 1952. The origin of metamorphic and metasomatic rocks. Univ. Chicago Press.

Robertson (E. C.), Birch (F.), and Macdonald (G. J. F.), 1957. Experimental determination of jadeite stability relations to 25 000 bars. Amer. Journ. Sci., vol. 255, p. 115.

Sundius (N.), 1918. Beiträge zur Kenntnis der Skapolithe. Bull. Geol. Inst. Univ. Upsala, vol. 16, p. 96.

Tilley (C. E.), 1937. The paragenesis of kyanite-amphibolites. Min. Mag., vol. 24, p. 555.

Turner (F. J.) and Verhoogen (J.), 1951. Igneous and Metamorphic Petrology. New York, McGraw-Hill Book Co., Inc.

New techniques for the universal stage.

I. An extinction curve method for the determination of the optical indicatrix.

By N. Joel, M.Sc., A.Inst.P.

Crystallographic Laboratory, Cavendish Laboratory, University of Cambridge

and

I. D. Muir, B.A., Ph.D., F.G.S.

Dept. of Mineralogy and Petrology, University of Cambridge.

[Read 6 June 1957.]

Summary. This paper describes a development for the universal stage of the extinction curve method for determining the orientation of the optical indicatrix in biaxial crystals. The extinction curve may be defined as the locus of the poles of the extinction directions when the crystal is rotated between crossed polarizers about an arbitrary but fixed axis perpendicular to the microscope axis.

When two or more extinction curves, or parts of them, are plotted on a stereographic projection, their intersections give the directions of the axes of the indicatrix, of which at least two are directly accessible. The main application of this new orthoscopic method is to provide a means of refining the orientation of the indicatrix obtained by this or any other method. The accuracy that can be obtained for minerals of low birefringence such as the felspars is considerably greater than with the conventional orthoscopic method.

A complete account is given of the details of the plotting procedure.

THIS is the first of several papers devoted to the use of the universal stage. The topics discussed are concerned mostly with the development of new or improved orthoscopic methods, which may be applied widely to rock-forming minerals in thin sections. In these papers, written for use with 3- or 4-axis universal stages, the nomenclature used for referring to the different rotation axes is that of Berek (1924) for the 4-axis stage.

One of the inherent difficulties in the conventional orthoscopic method of locating accurately the orientation of the indicatrix in biaxial crystals lies in determining how accurately the optic symmetry planes have been set normal to the A_4-axis of the universal stage. Conoscopic

methods afford a much higher degree of accuracy but can only be applied under favourable conditions.

The difficulties involved in the accurate location of an optic symmetry plane when corrections are required for refractive index differences between crystals and hemispheres have been discussed by Berek (1949) and by Hallimond (1950), who have described procedures whereby the plane may be located more accurately. Even where no refractive index correction is involved, however, the extinction position at any general inclined setting of the universal stage can always be determined with much greater precision than that with which an optic symmetry plane can be located by the orthoscopic method. This is because the extinction positions are determined by rotating the microscope stage for fixed settings of the inclined circles of the universal stage; whereas the orthoscopic setting of an optic symmetry plane is determined by extinction or near extinction being maintained as the crystal is rotated through an arc about the A_4-axis. Errors of the order of two degrees or more in the tilt of A_2, or of a degree or more on A_1 if A_2 has a high inclination, may still result in a state of near-extinction being observed on rotation about A_4. Therefore, if the axes of the optical indicatrix could be derived from the plotting of a series of accurately determined extinction positions, a considerable advance would be made in the accuracy that could be obtained by the use of orthoscopic methods with the universal stage.

Joel (1950, 1951), and Joel and Garaycochea (1957), using the simple microscope-stage goniometer of Bernal and Carlisle (1947), showed how the extinction curve of a crystal could be used to determine the orientation of the optical indicatrix of both uniaxial and biaxial crystals. It is shown here that extinction curve methods can be applied very successfully to the universal stage and that, because more than one horizontal rotation axis can be selected, ambiguities that are present in the method as originally described can be removed by using the universal stage. The method also becomes simpler.

Because the plotting of the extinction directions on a stereographic projection is not a very simple procedure, the method to be presented here cannot be described as a rapid one. Its principal application consists in refining the directions of the axes of the indicatrix, which may have been located approximately already by this or any other method. In certain circumstances, however, for example when working with finely twinned plagioclases, it provides a method of determining accurately the optic orientation where all other methods fail.

The extinction curve.

When a beam of light travels through a birefringent crystal in any direction except along an optic axis, there are two vibration directions associated with each wave normal. These are perpendicular to each other and to the wave normal, and when the crystal is observed between crossed polarizers they appear as the two corresponding extinction directions in the crystal.

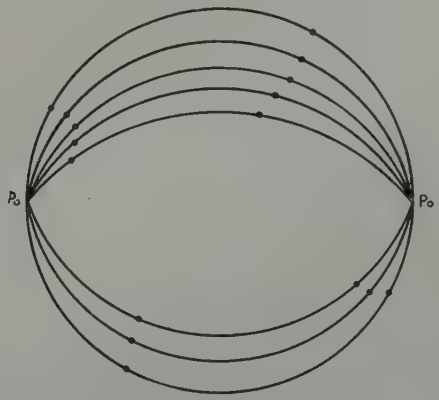

Fig. 1. One inclined great circle corresponds to each setting of the horizontal axis P_0. On each of these circles the poles of the extinction directions, obtained by rotating the stage about the microscope axis, are plotted. The extinction curve is the locus of these poles.

Consider now a crystal mounted on a stage free to rotate not only about the microscope axis but also about a horizontal axis perpendicular to it. For each setting on the horizontal axis it will be possible, by rotating the stage about the microscope axis, to determine the corresponding extinction directions. If this is done for a series of settings of the horizontal axis, and the extinction directions are inserted on a stereographic projection (fig. 1), then the poles thus obtained will lie along the 'extinction curve'.

The extinction curve can thus be defined as the locus of the poles of the extinction directions when the crystal is rotated between crossed polarizers about an arbitrary but fixed axis that is set perpendicular to the microscope axis. As can be seen, it can be represented very conveniently on a stereographic projection.

The generation of the extinction curve can be visualized in the follow-

ing way: P_0 is a point on the surface of an ellipsoid (the optical indicatrix) whose centre is O, and a diametral plane passes through OP_0. This plane intersects the ellipsoid along an ellipse whose axes D_1 and D_2 pass through the surface of the ellipsoid at four points, E_1, E_1', E_2, and E_2'. The locus of these points E when the diametral plane rotates round the line OP_0 is the extinction curve. Defined in this way, the extinction curve lies on the ellipsoid; but it can now be projected radially on to a sphere, and then to a stereographic projection.

The most important property of the extinction curve is the following: the poles of all the principal vibration directions of the indicatrix (X, Y, and Z for a biaxial crystal; the optic axis and all directions perpendicular to it in a uniaxial crystal) lie on the extinction curve. This is evident because when the crystal is rotated about its fixed horizontal axis, each of the principal vibration directions must in turn come into the plane of the microscope stage, and when this occurs they will become one of the two principal axes of that ellipse. It is because the poles X, Y, and Z lie on the extinction curve that it may be used to determine the orientation of the indicatrix.

Before a general description of the extinction curve is given, some simple cases will be considered.

Suppose, first, a uniaxial crystal with its optic axis perpendicular to the microscope axis is rotated about this optic axis. To obtain extinction the stage has to be rotated until the optic axis is parallel or perpendicular to the vibrations transmitted by the polarizer. If the crystal is now rotated about its horizontal axis P_0 (the optic axis), extinction will be maintained throughout. In this very special case the extinction curve consists of a great circle (the circular section of the ellipsoid, locus of ordinary vibration directions) and a point (the point P_0, pole of the optic axis, extraordinary vibration direction).

Consider now the same uniaxial crystal, but set in such a way that the rotation axis P_0 is no longer parallel or perpendicular to the optic axis. For any setting of the crystal about P_0, one of the two vibration directions will always have a refractive index ω (ordinary vibration), and the corresponding extinction directions will all lie in the circular section of the indicatrix. Thus, the extinction curve will still show a great circle (but inclined to P_0). The poles of the extraordinary extinction directions will lie on a curve that passes through the poles of the optic axis and of the rotation axis P_0, and the size of this curve will increase with the angular distance between these two poles (fig. 2). The complete extinction curve consists of three branches.

In the simplest case for a biaxial crystal, X or Z coincides with P_0 (the case where Y is parallel to P_0 will be considered later). If the crystal is set to extinction by rotation about the microscope axis, X or Z (and hence P_0) will be parallel or perpendicular to the vibrations transmitted by the polarizer. If a subsequent rotation is made about the horizontal

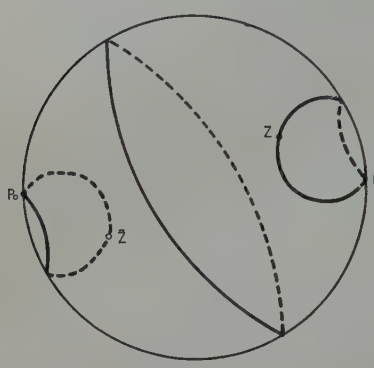

FIG. 2.

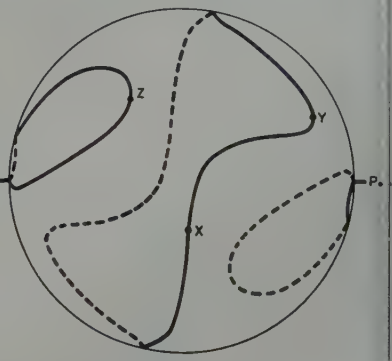

FIG. 3.

FIG. 2. Extinction curve of a uniaxial crystal, when Z is inclined to P_0.
FIG. 3. Extinction curve of a biaxial crystal ($CuSO_4.5H_2O$, triclinic) for rotation about a given axis P_0. X, Y, and Z are the principal directions of the indicatrix. In this particular setting the equatorial curve passes through X and Y, while the polar curve passes through Z and P_0.

axis the crystal will remain in extinction. Hence, the extinction curve will consist of a great circle and its poles (the poles of X or Z).

From the properties of an ellipsoid it follows that if the axis of rotation P_0 does not coincide with one of the three principal axes, the large curve will no longer be a great circle but will be a centrosymmetrical curve deviating somewhat from it by an amount that depends on the direction of P_0 relative to the indicatrix. And the locus of the other extinction direction (90° away from the first) will no longer be restricted to a point but will be a small curve.

For any given general direction of the rotation axis, the complete extinction curve (if both upper and lower poles are plotted) will consist of three branches: a curve encircling the sphere of projection and which is itself centrosymmetrical—this is the 'equatorial curve'; and two smaller curves, whose largest angular diameter never exceeds 90°; these curves, which are mutually symmetrical relative to the centre of the projection sphere, are the 'polar curves' (fig. 3).†

† Because of the symmetry of the extinction curves, all stereograms in this paper, except figs. 2 and 3, show the upper half of the projection only.

If the dihedral angles formed by the planes of the two circular sections are considered, the polar curves are confined to one pair of opposite angles (the ones that contain the rotation axis P_0) and the equatorial curve is confined to the other pair. Hence, the polar curves do not intersect the circular sections, while the equatorial curve does so, but only at their common intersections Y and $\bar{Y}$. Consequently, the equatorial curve always contains the poles of two axes of the indicatrix, one of which is Y. The pole of the third axis of the indicatrix, and also the point P_0, are on the polar curve.

On rotation of the indicatrix about a horizontal axis, the refractive indices associated with the two vibration directions fall into two groups, one limited to the range α to β, and the other to the range β to γ. One of these ranges is always fully covered, and corresponds to the equatorial curve; the other does not necessarily reach the β end of the range, and corresponds to the polar curve. For instance, if X is on the polar curve, then Y and Z will be on the equatorial curve, and in this case all the points of the latter will correspond to vibrations with refractive indices in the full range β to γ.

When Y, or indeed any direction lying in either of the two circular sections, is set parallel to the rotation axis, a limiting case arises: the equatorial and polar branches of the extinction curve touch at four singular points on the same circular section. The extinction curve includes this circular section in such a way that one half is covered by the equatorial curve and the other half by the polar curves. In this case it becomes difficult to distinguish by simple inspection between the equatorial and the polar parts of the curve.

For the particular case of the Y-axis coinciding with the horizontal rotation axis, the whole extinction curve now consists of the great circle XZ and the two circular sections of the indicatrix. This is due to the fact that throughout the rotation positions are reached in which the crystal is being observed along each of its optic axes. These considerations apply also to uniaxial crystals when the rotation axis P_0 lies in the circular section of the indicatrix. The extinction curve then consists of the circular section and a great circle perpendicular to P_0.

Examples of extinction curves, details of their use with a one-axis stage, and a brief mathematical treatment of the problem have been given by Joel and Garaycochea (1957). They showed how the orientation of the indicatrix of biaxial crystals could be determined by locating on the extinction curve three points 90° distant from each other. Two such triangles are obtained in the general case, the 'true' triangle and

a 'ghost' triangle. Criteria were given by which the 'true' triangle XYZ could always be distinguished from the 'ghost' one. The accuracy with which X, Y, and Z can thus be located, that is, the precision with which a tri-rectangular spherical triangle can be located with its vertices on the extinction curve, depends greatly on the shape of the extinction curve which in turn depends on the direction of the rotation axis relative to the indicatrix.

Johannsen (1918) refers briefly to an extinction curve in his extensive review of methods for the graphical determination of zonal extinction angles and their use in such problems as plagioclase determination, but he makes no attempt to use them. It is clear from the discussion of Duparc and Pearce (1907) that the use of these extinction curves for determining the orientation of the optical indicatrix was not known to the early workers in crystal optics.

Application of extinction curves to the universal stage.

The extinction curve method was applied originally to a one-axis microscope-stage goniometer which can be compared to a universal stage in which the A_4-axis only is used. This instrument is very suitable for the microscopic examination of a mineral grain mounted on a fibre such as would be used for single-crystal X-ray work, and it permits a complete rotation of the crystal about the horizontal axis.

Clearly this method can be applied to a universal stage. If the A_4-axis alone were used, the universal stage would be at a disadvantage owing to the limited rotation about A_4, but use can be made of other axes. It is here that the new developments in the extinction curve method arise, and with the universal stage the method can now be applied to thin sections as well as to grains.

The methods described here refer only to biaxial crystals, for the uniaxial case is simple, and are applied to a 4-axis universal stage. The operations carried out during the procedure involve the determination of a number of extinction directions and the plotting of two or more extinction curves. The method is based on the fact that more than one horizontal rotation axis may be selected. The extinction curve is drawn for each of these axes. Since the poles X, Y, and Z must lie on each extinction curve, they will be determined by the intersections of the different extinction curves.

For any given rotation about the A_4-axis, the inaccessible region due to the restriction on the rotation will be the area shown in fig. 4*a*. However, any pole in this region inclined at more than about 30° or 35° to the

normal of the section can be made accessible by a suitable rotation about the A_3-axis, as shown in fig. 4*b*, to bring it near the N.–S. plane. In this way the inaccessible region is reduced to the area lying within a small circle concentric with the pole of the section and of angular radius 30° to 35°. This is referred to as the 'blind circle'.

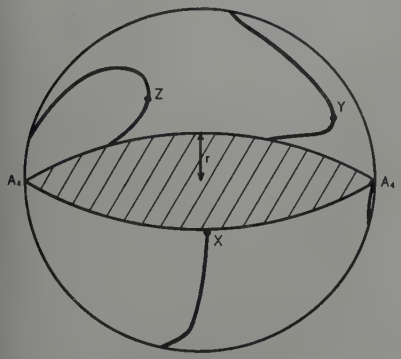

FIG. 4*a*.

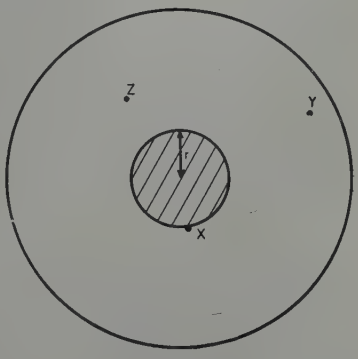

FIG. 4*b*.

FIG. 4*a*. Same crystal and same setting as in fig. 3. Owing to the restriction on the rotation about A_4, extinction directions within the shaded area of the projection become inaccessible; $r = 30°$ to 35°.

FIG. 4*b*. Same crystal as in figs. 3 and 4*a*. By making use of other axes of the universal stage, the inaccessible region is reduced to the 'blind circle'; $r = 30°$ to 35°. At least two of the three principal directions of the indicatrix always lie outside the 'blind circle' and hence are accessible.

As the 'blind circle' cannot contain more than one of the points *XYZ*, two of the axes and sometimes all three of them can be located directly by means of the extinction curves.

In the following sections the terms α_1, α_2, α_3, α_4, α_5 are used to define the angular rotations about the respective axes from their zero positions. For A_1, A_3, and A_5 (microscope stage axis) the divided scales are marked in such a way that clockwise rotations increase their readings (the zero reading on A_3 is 90°); hence, for these axes the α angles define a clockwise rotation from the zero setting. Readings on A_2 are made on the left- or right-hand arcs according to the tilt on that axis. Readings on this axis are therefore recorded $\alpha_2 L$ or $\alpha_2 R$. Similarly for A_4; readings are recorded as $\alpha_4 N$ (stage inclined towards the observer) and $\alpha_4 S$ (stage inclined away from the observer).

In the procedure that follows, the inner axes of the stage, A_1 and A_2, may be used in certain circumstances, such as for finely twinned plagioclases, to set the crystal into a more desirable orientation for determining

the extinction curve. Once these axes have been set, their positions should not again be altered until the operations have been completed. All subsequent operations are carried out using the outer axes A_3, A_4, and A_5. If there is no need to incline the section ($\alpha_2 = 0$), then A_1 may be used for those parts of the procedure described here for A_3 and the technique may then be used with a 3-axis stage, or indeed a 2-axis stage. The 3-axis stage can be used for all the operations described here, but if it is necessary to incline the A_2-axis, the plotting becomes very complex and it is recommended that such operations should always be carried out on the 4- or 5-axis instruments. For the 5-axis stage the additional axis (inner east–west) is not required for the extinction curve procedure.

Procedure.

The use of the outer axes ($\alpha_2 = 0$). All axes of the stage are set to their zero positions, and the crystal to be examined is brought to the centre of the field. A_1 is set to a convenient position and its reading is noted. If there should be no preference for any particular position of A_1, it is best to begin with $\alpha_1 = 0$.

Rotate the crystal to extinction by a clockwise rotation on A_5; record the α_5 angle ($\alpha_4 = 0$); these extinction directions will later be inserted on the stereogram as four points on the primitive.

Rotate A_4 to 10° N., adjust A_5 to extinction again, and note the α_4 and α_5 values.

Make further successive rotations of 10° on A_4 to cover the complete available arc of rotation and for each setting note the α_5 extinction angle. When these readings are plotted on the upper hemisphere of the projection, each A_4 setting will produce two poles 90° apart on the respective great circles which represent planes inclined to the section at angles corresponding to the $\alpha_4 N$ or S values.

When sufficient extinction directions have been obtained for the particular setting of A_3 they are plotted as described below, and the accessible portion of the extinction curve is drawn through these poles.

A new rotation axis is now selected in order to obtain a second extinction curve. This can be done in a variety of ways, two of which do not involve complicated plotting: if the A_4-axis is set to its zero reading the second rotation may be performed about A_2; this enables a rotation to be made about an axis perpendicular to the first one. Or if A_2 is left fixed at its zero reading, the rotations may be performed around the A_4-axis after rotating the A_3-axis into a new position. In this way any

rotation axis in the plane of the section can be selected, and by further rotations about A_3 as many additional extinction curves may be obtained as are desired (fig. 5). No definite rules can be given as to the new settings of A_3 that will produce good intersections of the extinction curves, but

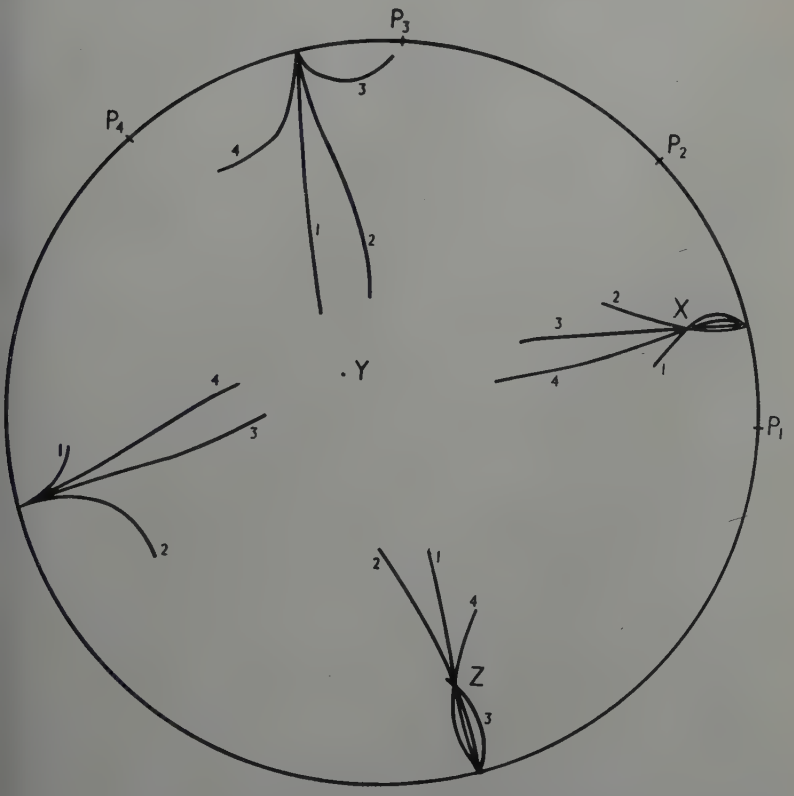

FIG. 5. Four extinction curves for a specimen of labradorite from porphyritic basalt, St. John's Point, County Down. P_1, P_2, P_3, and P_4 are the poles of the rotation axis A_4 for settings of A_1 equal to 0°, 45°, 90°, 135°; and the numbers by the curves indicate the corresponding rotation axis. The parts of the curves that point towards Y are the equatorial curves.

(as can be seen in fig. 5) a rotation of A_3 of 45°, 90°, 135°, or intermediate values, will usually produce satisfactory results.

After two extinction curves have been recorded and the three axial points have been located, a process of refining their positions may be carried out; indeed, the conventional orthoscopic procedure could be used at first to locate these points approximately. For each of the

rotation axes selected, the regions close to the poles of the accessible indicatrix axes are explored and the extinction curves plotted in smaller steps of rotation about A_4.

After the three indicatrix axes have been located, they are identified in the usual manner by means of the compensating plates. It is useful to remember at this stage that the Y-axis always lies on the equatorial curve; even with the incomplete extinction curves obtained on the universal stage it is usually possible to distinguish between their equatorial and polar parts.

It should be noted that if the rotation axes are chosen so that they all lie in the same plane, which is generally the case, then the different extinction curves will have two additional points of intersection in the upper hemisphere, both of them in that same plane. If $\alpha_2 = 0$ throughout, these additional intersections will occur at four points on the primitive. Their presence should not cause any ambiguity. These points might be considered to be 'shadows of the ghosts'.† They need not occasion any alarm.

Use of the inner axes ($\alpha_2 \neq 0$). If it should be desired to set the crystal into a more convenient position for its rotation, use can be made of the inner axes A_1 and A_2. This would arise, for instance, if a cleavage plane or twin composition plane should be kept vertical during the rotation. Such preliminary settings are particularly desirable when dealing with finely twinned plagioclase where any considerable obliquity of the composition plane may cause the walls of contiguous lamellae to overlap and prevent the extinction positions from being determined. In this way the extinction curve and 'zonal' methods of plagioclase determination may be carried out simultaneously. In the case of normal twins the requirement for extinction angles in adjacent lamellae to be equal and opposite when the composition plane is vertical affords a check on the measurements. Other cases where it may be desirable to incline the A_2-axis arise when a grain to be examined has an optic axis nearly vertical; the low partial birefringence at low inclinations of A_4 then makes an exact determination of the extinction positions difficult.

The procedure when the A_2 circle is inclined is as follows:

By means of A_1 set the crystal in the desired orientation, e.g. set the trace of the composition plane parallel to the N.–S. crosswire. Using A_2, set the composition plane vertical.

Set to extinction on A_5; as before, A_4 is used as rotation axis.

When further extinction curves are required these may be obtained

† See Joel and Garaycochea, 1957, p. 401.

by altering the setting of A_3. The composition plane will no longer be N.–S., nor will it remain vertical, but by selecting suitable rotations about A_3 it can be made to deviate less from the vertical than if A_2 had not been inclined.

Plotting.

With a 4-axis universal stage and a rotating-stage microscope there are five axes of rotation available. In their zero positions three axes are vertical (A_1, A_3, A_5) and two are horizontal (A_2, A_4). The graduated circles of the first three are marked in such a way that clockwise rotations increase their readings. For the actual plotting, the stereographic net should be placed with its inclined great circles running E.–W.

The zero of A_1 is the south point of the primitive, and the zero setting of the A_3-axis (which reads 90°) is the west point. Therefore, for plotting the extinction directions, the tracing paper must first be rotated to a position corresponding to the reading on A_1; that is, a clockwise rotation equal to α_1. In the plotting, the zero of the paper is rotated to the appropriate reading of A_1 or (if $\alpha_2 = 0$) of A_3. All the other readings are made then along the fixed circles inscribed on the net.

First set the tracing paper over the net and mark on it a point S_1 coinciding with the south point of the primitive and a point W_3 coinciding with the west point of it. The former is to be used as origin for the readings of A_1 and the latter for those of A_3 (provided $\alpha_2 = 0$). In both cases the paper should be turned clockwise.

As the plotting procedure is more involved when the A_2 circle is inclined than when it is on its zero position, the two cases will be dealt with separately.

If $\alpha_2 = 0$. Since the axis A_4 is E.–W., its readings are inserted on the tracing paper along the N.–S. great circle of the net: readings for tilts north (towards the observer) are inserted inwards from the south point of the primitive, that is, towards the north; and conversely for rotations in the opposite sense.

Rotations about A_4 bring the inclined great circles running E.–W. successively into positions perpendicular to the microscope axis. Therefore, after the appropriate great circle has been selected according to the A_4 reading, the extinction directions—as read on A_5—are inserted along it.

The zero position of A_5 is the one in which the A_4-axis runs E.–W. And it is the difference between the actual readings of A_5 at extinction and its zero-position reading that are relevant and constitute the α_5

angles. For the purpose of inserting the extinction directions into the stereogram, positive values of α_5 only need be considered; it is always possible to add or to subtract any multiple of 90° to the A_5 reading, and thus to restrict the values of α_5 to the range 0° to 180°. This simplifies the plotting.

The values of α_5 thus obtained are inserted along the appropriate

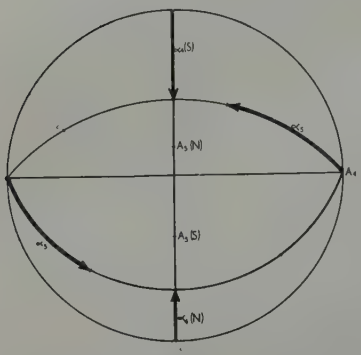

FIG. 6*a*.

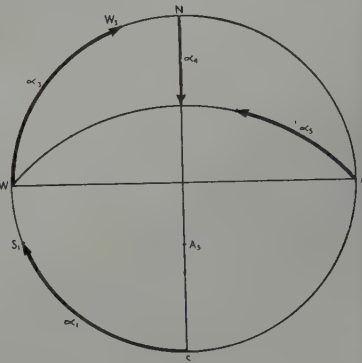

FIG. 6*b*.

FIG. 6*a*. Two examples of plotting: $\alpha_1 = \alpha_2 = \alpha_3 = 0°$; $\alpha_4 = 20°$ N, $\alpha_5 = 50°$
$\alpha_1 = \alpha_2 = \alpha_3 = 0°$; $\alpha_4 = 40°$ S, $\alpha_5 = 60°$.

FIG. 6*b*. Example of plotting with $\alpha_1 \neq 0°$; the tracing paper has been rotated clockwise, through an angle equal to α_1 before inserting α_4 and α_5. $\alpha_1 = 70°$, $\alpha_2 = \alpha_3 = 0°$, $\alpha_4 = 40°$ S, $\alpha_5 = 60°$. In fact the same plotting will be obtained in this case ($\alpha_2 = 0°$) if $\alpha_1 = 0°$ and $\alpha_3 = 70°$, or indeed for any α_1 and α_3 such that $\alpha_1 + \alpha_3 = 70°$.

inclined great circle. For north tilts of A_4 the readings are made anti-clockwise along the great circles from the west point of the primitive; for south tilts, anticlockwise from the east point (fig. 6).

If $\alpha_2 \neq 0$. When it has been necessary to use the two inner axes the plotting becomes more difficult. If by means of A_1 the trace of a plane has been set N.–S., this position of A_1 should be taken as its zero position (the point S_1 of the stereogram coinciding with the S point of the net). It should not be altered during the rest of the procedure. Then the plane was set vertical by means of A_2. Fig. 7*a* shows the pole of A_4 for $\alpha_2 = 30°$ L (the normal to the section is tilted 30° to the right). Rotation about A_4 will in turn bring parallel to the microscope stage planes represented by great circles through this new position of A_4 (which is not the point E of the net). Fig. 7*a* shows one of these great circles along

which α_5 has to be inserted. Fig. 7*b* shows the plotting for a case in which all five axes have been used.

The plotting of this case can nevertheless be simplified considerably if it is carried out first as if α_2 and α_1 were zero. α_3 readings are inserted around the primitive, α_4 along the line N.–S., and α_5 along the inclined

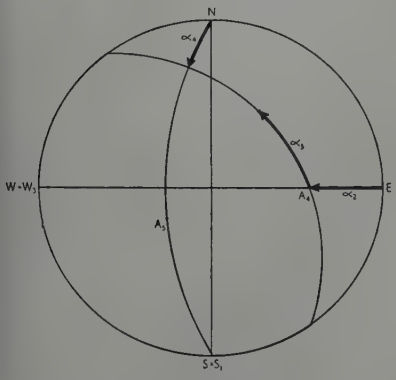

FIG. 7*a*.

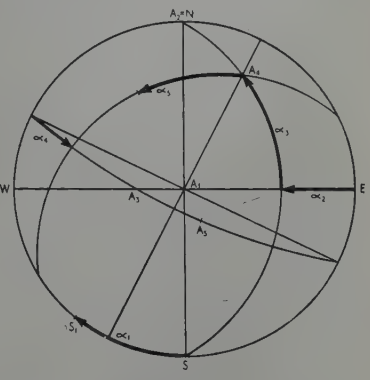

FIG. 7*b*.

FIG. 7*a*. Example of plotting with $\alpha_2 \neq 0°$: $\alpha_1 = 0°$, $\alpha_2 = 30°$ *L*, $\alpha_3 = 0°$, $\alpha_4 = 20°$ S, $\alpha_5 = 50°$.

FIG. 7*b*. Example of plotting in the most general case: $\alpha_1 = 40°$, $\alpha_2 = 30°$ *L*, $\alpha_3 = 60°$, $\alpha_4 = 20°$ S, $\alpha_5 = 50°$.

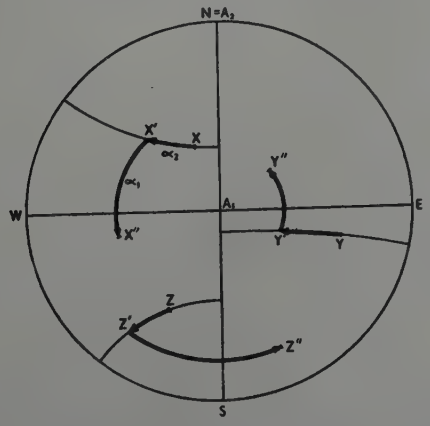

FIG. 8. *X*, *Y*, and *Z* are the poles of the axes of the indicatrix obtained by neglecting the A_1 and A_2 readings in the plotting. A rotation of amount α_2 about A_2 brings them to *X'*, *Y'*, and *Z'*. A further rotation of amount α_1 about A_1 brings them to *X''*, *Y''*, and *Z''*, which are the poles of the axes of the indicatrix referred to the plane of the mineral section. In this example $\alpha_1 = 60°$ and $\alpha_2 = 30°$ *L*.

great circles just as before. When the positions thus obtained for the poles X, Y, and Z have to be referred to the zero setting of the section, this can be done by rotating them around the N.–S. line of the stereogram (they will move along small circles perpendicular to this line) by an angle equal to α_2 (to the left if α_2 was a reading on the left), and then by rotating them about the centre of the stereogram by an angle equal to α_1 in an anticlockwise sense; fig. 8 shows this.

Corrections.

The *corrections* due to inclined incidence when the refractive indices of crystal and hemispheres are different can be applied very simply if the crystal has a low birefringence. Its estimated average index can then be used for the correction.

If $\alpha_2 = 0$, the only correction necessary is the one to be applied to α_4. The plotting is made easier if instead of applying the correction to the stereogram it is made to the A_4 setting of the stage, in the opposite sense, in order to make use of one of the great circles drawn on the net.

If $\alpha_2 \neq 0$, the angle to be corrected is α', given as usual by $\cos \alpha' = \cos \alpha_2 . \cos \alpha_4$. And the correction has to be applied radially towards (or away from) the pole of the normal to the section. Both the determination of α' and the actual correction should be made on the stereogram in the customary way. More details on these corrections, especially for crystals of high birefringence, are given by Joel and Muir (1958).

Accuracy of measurements with the universal stage.

With the standard orthoscopic method it is difficult to check on the accuracy with which the optic planes have been set. A check can be applied to the setting of the optic axial plane by rotating the A_5-axis into the alternative 45° positions and testing the locations of the optic axes, but no check can be applied to the other two optic symmetry planes except that the three axes of the indicatrix should be 90° distant from each other. Errors of two or three degrees in the location of XYZ are not uncommon. The use of twin crystals affords in many cases a reliable check on the accuracy with which the principal vibration directions XYZ have been located in both subindividuals, but if only two twin subindividuals have been plotted and if the plotted poles of any pair of equivalent principal vibration directions lie within about 20° or less of each other, then a very small error in location of one of them may greatly affect the determination of the position of the twin axis. Also

compensating errors may well hide inaccuracies in the location of XYZ in one or both subindividuals.

A high degree of accuracy may be obtained when it is possible to use conoscopic methods; these may be used satisfactorily in thin sections with minerals of high birefrigence such as olivine, provided that the crystals are of sufficient size and unzoned, and that fine twin lamellae are not present. If the mineral has a high refractive index, the upper surface of the section should be polished to avoid irregular refraction of the emergent rays. Conoscopic methods used with grains can also be applied to minerals of relatively low birefringence such as the alkali felspars. In favourable cases the points of emergence of the optic axes may be located with an accuracy of about 0·5°. Where fine twin lamellae are present or the mineral is strongly zoned, conoscopic methods cannot be used.

One of the commonest uses of the universal stage is for the determination of the composition and assessment of the structural state of the plagioclase felspars. In many cases, both the composition and the structural state may be estimated with a reasonable degree of accuracy if the mineral is not too strongly zoned or if the twin lamellae are sufficiently broad to make possible accurate orthoscopic settings of the optic symmetry planes. The optical distinctions between 'high' and 'low' natural plagioclases are greatest for albite and diminish as the anorthite content increases. Because of this, the distinctions can be made most readily for minerals more sodic than An_{40}. Felspars whose compositions lie between An_{15} and An_{40} frequently exhibit both strong zoning and fine twinning. Such felspars cannot be determined satisfactorily using the normal orthoscopic method. To meet these difficulties, Rittmann (1929) developed the 'zonal' method in which the universal stage was used to orient the crystal into the most convenient position for the measurement of its extinction angles in the conventional petrographic manner. This method has the advantage of being simple and rapid and gives very satisfactory results where the plagioclase is known to be in a low state. For plagioclases thought to be in a transitional or natural high state, however, a determination of refractive index (Schwarzmann, 1955) is required in addition to the measurements of the Rittmann method. These difficulties do not arise if the extinction curve method can be used to determine accurately the optical orientation of the various subindividuals of a twinned crystal.

With the extinction curve method any inaccuracies of measurement are shown up immediately by the course of the curves as the plotting

proceeds. If more than two curves are plotted they should all intersect in the poles XYZ; any inaccuracy of measurement can be estimated by the departure of these curves from concurrence. The accuracy that can be obtained depends on the accuracy with which extinction can be set, and this in turn depends on the birefringence and optic axial angle of the mineral. For minerals of very low birefringence the setting of extinction can be improved considerably by the use of a low-power objective and a Nakamura twin-crystal plate with a cap analyser.

In the case of the plagioclase felspars the locations of XYZ could be determined with an accuracy estimated to be of the order of about one degree. This is considerably better than could be obtained with the conventional orthoscopic procedure.

The example shown in fig. 5 is a favourable one as the extinction settings could be made readily. Even in less favourable cases, however, accurate results can be obtained because it is possible to choose several rotation axes in the crystal and so to plot as many extinction curves as are required.

Conclusions.

Although the method described in this paper is not a rapid one, the plotting, which is the only difficult part of the procedure, can be done quite rapidly once the operator has become familiar with it; the method then requires only about twice the time demanded by the normal procedure of plotting optic symmetry planes. The amount of plotting required may be reduced considerably if the positions of the axes of the indicatrix can be located approximately first, for then only those portions of two or more extinction curves that are adjacent to the axial points need be determined. Applied in this way the method is very useful for refining the orientation of the indicatrix, especially so for minerals of low birefringence.

When applied to finely twinned plagioclases it provides the only method whereby the optical orientation may be obtained, but even this method may fail with very finely twinned plagioclases such as those from the rhomb porphyries.

The positions of the optic axes cannot be located directly by the extinction curve method, nor can it be used for determining directions lying within the 'blind circle', but this is the region where the normal orthoscopic procedure of determining optic symmetry planes can be applied with the most accurate results. Finally, it should be pointed out that the conventional orthoscopic method of setting an optic symmetry

plane of the indicatrix normal to the A_4-axis of the universal stage is a special case of the more general extinction curve method presented here.

Acknowledgements. The authors wish to express their gratitude to Prof. C. E. Tilley, Dr. W. A. Wooster, and Dr. N. F. M. Henry for their interest in the progress of this work, and to Dr. Henry for his careful reading of the manuscript and his most helpful and constructive advice and criticism of the presentation. One of us (N. J.) carried out this work during tenure of a research grant from the British Council, assistance now gratefully acknowledged.

References.

Berek (M.), 1924. Mikroskopische Mineralbestimmung mit Hilfe der Universaldrehtischmethode. Gebrüder Borntraeger, Berlin.
—— 1949. Schweiz. Min. Petr. Mitt., vol. 29, p. 1.
Bernal (J. D.) and Carlisle (C. H.), 1947. Journ. Sci. Instrum., vol. 24, p. 107.
Duparc (L.) and Pearce (F.), 1907. Zeits. Kryst. Min., vol. 52, p. 37.
Hallimond (A. F.), 1950. Mining Mag., vol. 83, pp. 12, 77 [M.A. **11**–281].
Joel (N.), 1950. Min. Mag., vol. 29, p. 206.
—— 1951. Ibid., p. 602.
—— and Garaycochea (I.), 1957. Acta Cryst., vol. 10, p. 399.
—— and Muir (I. D.), 1958. Min. Mag., vol. 31, p. 878.
Johannsen (A.), 1918. Manual of Petrographic Methods, 2nd edn, pp. 406–412. McGraw-Hill Book Co., New York.
Rittman (A.), 1929. Schweiz. Min. Petr. Mitt., vol. 9, p. 1 [M.A. **5**–282].
Schwarzmann (S.), 1956. Heidelberger Beitr., vol. 5, p. 105.

New techniques for the universal stage.

II. The determination of 2V when only one optic axis is accessible.

By N. Joel, M.Sc., A.Inst.P.

Crystallographic Laboratory, Cavendish Laboratory, University of Cambridge

and

I. D. Muir, B.A., Ph.D., F.G.S.

Dept. of Mineralogy and Petrology, University of Cambridge.

[Read 6 June 1957.]

Summary. When one optic axis of a biaxial crystal has been located accurately by the usual orthoscopic or conoscopic methods, the second may be located by determining the extinction positions at normal incidence and applying the Biot–Fresnel construction. When use is made of the extinction directions associated with two or more wave normals inclined to the section, this method gives more reliable values of the optic axial angle than can be obtained by the doubling of the angle V over the pole of a bisectrix. If the optic axes have been located with sufficient accuracy by this procedure, then this also determines the orientation of the indicatrix.

WHEN one optic axis and a bisectrix of a biaxial crystal have been located, it is customary to obtain the second optic axis by doubling the angle V over the bisectrix. This procedure, to which resort must frequently be made when the optic axial angle is large, is liable to give inaccurate values for $2V$ (errors of 2° to 5° are not uncommon), because the position of the first optic axis, or the bisectrix, or possibly both, may not have been determined with the requisite accuracy.

As the Biot–Fresnel construction may be used to determine the two vibration directions associated with any given wave normal within a biaxial crystal when the orientation of the wave normal is known relative to the optic axes, it may be used to check on the accuracy of the observations when both optic axes have been determined. This method can be applied if the two extinction directions associated with a given wave normal are known. For this purpose it is customary to use the wave travelling normally to the section. The extinction directions

then would lie in the plane of the section (Hallimond, 1950 and 1953). Fig. 1 shows how this procedure is carried out on a stereographic projection.

This application of the Biot–Fresnel construction becomes inaccurate when the optic axial plane is nearly vertical and indeterminate when this plane is vertical. When the plane is nearly vertical, a very slight error in the determination of the first optic axis, the optic axial plane, or the extinction positions, can lead to a very considerable error in the derived position of the second optic axis. By inclining the section, however, this difficulty can be overcome (Hallimond, 1953), as several more suitable wave normals inclined to the plane of the section may be chosen and their associated extinction directions determined. In this way greater accuracy may be obtained and the method will always provide a satisfactory check on the location of the second optic axis when one bisectrix and one or both optic axes have been determined in the usual way.

The accurate location of the first optic axis. If one optic axis of a biaxial crystal can be determined accurately, the Biot–Fresnel construction may be used to determine the second optic axis, and hence the value of $2V$, with no other additional information than the pair of mutually perpendicular extinction directions associated with each of three or more wave normals. In order to save time in the choice of these wave normals, as they have to be sufficiently distant from the optic axial plane, it is convenient, though not necessary, to know the approximate orientation of this plane.

The success of this procedure depends greatly on the accuracy with which the first optic axis has been located. It is recommended, therefore, that after the optic axis has been made as vertical as possible by the orthoscopic procedure, an attempt should be made to locate its position more accurately by means of an interference figure. This can often be used with minerals of moderate birefringence, even if only an imperfect figure is obtained in other positions, for the isogyres are narrowest and most clearly defined in the vicinity of an optic axis. Consequently, there is a much greater chance of obtaining a useful interference figure from a grain in a thin section when in this orientation. The point of emergence of the optic axis can be recognized as the point about which the isogyre rotates when the microscope stage is revolved. The optic axis should be brought into coincidence with the axis of the microscope. If the optical system has been adjusted correctly, this latter direction should coincide with the centre of the conoscopic ring mark engraved on the back focal

plane of the objective. If no such ring mark is provided, the intersection of the cross wires may be used for this purpose if the Bertrand lens has been centred correctly.

If the first optic axis cannot be located by convergent light methods,

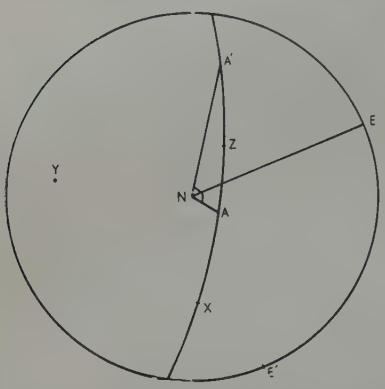

Fig. 1.

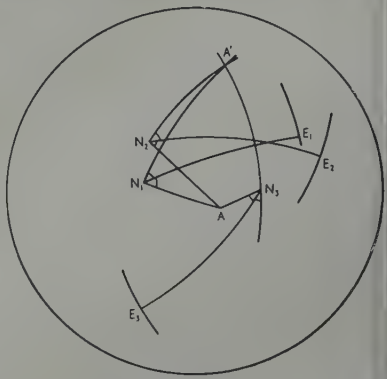

Fig. 2.

Fig. 1. The use of the Biot–Fresnel construction for locating the second optic axis. X, Y, and Z are the principal vibration directions, A is the optic axis which has been determined directly, E and E' are the extinction directions associated with the plane wave travelling normally to the section. An angle equal to $\widehat{ANE}$ is constructed on the opposite side of NE. The intersection of the great circle so obtained with the circle XAZ is the pole A' of the second optic axis. As a check, the arcs AZ and ZA' should be equal.

Fig. 2. The Biot–Fresnel construction applied to wave normals inclined to the section. (Crystal of labradorite from porphyritic basalt, St. John's Point, Co. Down.) One optic axis only, A, has been determined previously. By means of the three wave normals N_1, N_2, N_3, with their corresponding extinction directions E_1, E_2, E_3, the second optic axis is determined. As in fig. 1 an angle equal to the angle $\widehat{AN_1E_1}$ is constructed on the opposite side of N_1E_1. The same procedure is carried out using N_2 and N_3 with their corresponding extinction directions. The three great circles thus obtained intersect at A', the second optic axis.

use can be made of the 'optical curves' introduced by Fedorov (1896) and summarized by Johannsen (1918).

These optical curves may be obtained by the following procedure: All axes of the universal stage are set at zero, the nicols are crossed, and the A_4-axis is set parallel to the vibration plane of the polarizer or analyser. At successive inclinations of A_4, 0°, 10°, 20°, &c., N. and S., the crystal is set to extinction by a rotation of A_1. The wave normals corresponding to the pairs of readings (α_1, α_4) are then plotted on a stereogram. The locus of these points is the optical curve. These optical

curves, in which wave-normals are plotted, must not be confused with the extinction curves described by Joel and Muir (1958), in which vibration directions are plotted.

Further optical curves are now obtained by repeating the same procedure for different positions of A_4 relative to the crossed nicols. All such optical curves should intersect at the poles of the optic axes (and also at the pole of the normal to the section). If the accessible optic axis has first been located approximately, it is necessary to determine only those portions of the optical curves near this optic axis.

An alternative orthoscopic method of refining the position of the accessible optic axis is given by Turner (1942).

The determination of the second optic axis. Fig. 2 shows the extinction directions associated with three inclined wave normals plotted on a stereographic projection. Details of the plotting procedure for extinction directions obtained from wave normals inclined to the section are given by Joel and Muir (1958), pp. 871–874. Fig. 2 shows also how the different great circles (one great circle for each wave normal), drawn to locate the second optic axis, should intersect to give its position. In theory, the intersection of two such great circles should be sufficient to fix the position of this optic axis, but a good check can be obtained by using three or more of them. If these great circles depart significantly from a unique intersection, it must follow either that one or more of the pairs of extinction directions have been determined incorrectly, or that the first optic axis has not been located with sufficient accuracy.

Corrections. This method is most easily applied when no correction is required for refractive index difference between crystal and hemispheres. This applies for instance when both the maximum birefringence $\gamma-\alpha$ and the difference $|n_c-n_h|$ between the average index of the crystal n_c and that of the hemispheres n_h are less than about 0·03.

Where the necessity for refractive index correction arises, a distinction must be made between minerals of low and high birefringence:

With minerals of low birefringence, $\gamma-\alpha \ll |n_c-n_h|$, and the average index n_c of the crystal is used to estimate the correction. This correction is then applied to the pole of the wave normal in the usual way, radially towards or away from the centre of the stereogram, before actually plotting the extinction directions. These are then inserted along the corrected great circle.

With minerals of high birefringence, significant errors may be incurred by using an assumed average index for estimating the correction. Ideally, in this case, the correction to the wave normal should be applied

separately for the two vibrations, each with its correct refractive index. If these cannot be estimated by means of an approximate knowledge of the principal refractive indices and the orientation of the indicatrix, or by any other means, the average index n_c is still used. The errors involved in this approximation may be reduced by determining the extinction directions for a larger and randomly selected set of wave normals.

Conclusions. It is worth while stressing that the reliability of this method of determining the value of $2V$ lies in the fact that several arcs are required to intersect on (or very near to) a single point, which provides a good check. The same can be said of Fedorov's optical-curves method for determining the optic axis that is directly accessible. The combination of Fedorov's method and the one described in this paper should therefore lead to a determination of the two optic axes of great accuracy, limited only by the number of graphical constructions one wishes to make—in other words, by the time available to the observer.

It is interesting also to note that not only does this method lead to the determination of the second optic axis, and hence of $2V$, but it may be used to determine the actual orientation of the indicatrix quite independently of any other of the usual methods. The usefulness of this last application will depend, of course, on whether or not the error in the determination of the optic axes will be smaller than that of the conventional determination of the symmetry planes of the indicatrix, which may happen in some cases. Alternatively, it may be used as a check on the determination of the principal axes of the indicatrix.

Acknowledgements. The authors wish to thank Dr. N. F. M. Henry for his interest and helpful criticism of the manuscript. One of us (N. J.) wishes to express his gratitude to the British Council for a research scholarship.

References.

Fedorov (E.), 1896. Zeits. Kryst. Min., vol. 26, p. 225.

Hallimond (A. F.), 1950. Mining Mag., vol. 83, pp. 12 and 77 [M.A. **11**–281].

—— 1953. Manual of the Polarising Microscope, 2nd edn (York: Cooke, Troughton and Simms), p. 160.

Joel (N.) and Muir (I. D.), 1958. Min. Mag., vol. 31, p. 860.

Johannsen (A.), 1918. Manual of Petrographic Methods, 2nd edn (New York McGraw-Hill Book Co.).

Turner (F. J.), 1942. Amer. Journ. Sci., vol. 240, p. 571 [M.A. **8**–350].

SHORT COMMUNICATIONS

A further occurrence of phosgenite.

In a recent note Kingsbury[1] described two new localities for phosgenite in the United Kingdom. This mineral has some interest in building since it may be a corrosion product of lead materials in contact with chloride solutions. Opportunity was taken to establish the standard data when a sample found by Mr. G. W. Mack in an ancient lead pot deep in Wookey Hole was presented for study in 1948. The mineral occurs as flattened plates about $1 \times 1 \times 0{\cdot}3$ cm. maximum, colourless and for the most part clear. Chemical analysis by R. S. Gillett gave: PbO 81·2, Cl 12·6, CO_2 8·0 %, equivalent to $Pb_2(CO_3)Cl_2$. The crystals have refractive index about 2·15, uniaxial positive; crystallographically the most prominent face is *c* {001}; other forms identified include *u* {120}, *x* {111}, *m* {110}, *b* {010}, and *o* {021}. The material has the high specific gravity of 6·15. An X-ray powder diffraction pattern using filtered Co-$K\alpha$ radiation gave the following results:

d.	*I.*	*d.*	*I.*	*d.*	*I.*	*d.*	*I.*
5·71 Å.	w	2·40 Å.	vvw	1·800 Å.	m	1·402 Å.	vvw
4·40	s	2·28	vw	1·757	mw	1·393	vvw
4·04	ms	2·21	m	1·672	mw	1·364	w
3·61	vs	2·03	vw	1·636	vvw	1·352	w
3·50	vvw	1·97	mw	1·588	vvw	1·327	w
3·09	vvw	1·94	vvw	1·508	vw	1·294	mw
2·99	vw	1·91	mw	1·495	vvw	1·285	vvw
2·86	vvw	1·887	mw	1·469	mw	1·277	vvw
2·79	vvs	1·841	vvw	1·445	mw	1·267	vw
2·56	vs	1·820	vvw	1·426	m		

If the unit cell proposed by Oftedal[2] is taken as a guide, the data above give unit-cell dimensions *a* 8·112 Å., *c* 8·814 Å., $c/a = 1{\cdot}086$.

The formation of phosgenite under similar conditions has been reported by Lacroix from Maldia, Tunis,[3] where an ancient metallic object was immersed in sea-water, and also from Bourbonne-les-Bains, France,[4] where a lead pipe was exposed to a hot spring.

Building Research Station,
Watford, Herts.

H. G. Midgley

[1] A. W. G. Kingsbury, Min. Mag., 1957, vol. 31, p. 500.
[2] I. Oftedal, Norsk Geol. Tidsskr., 1945, vol. 24, p. 79.
[3] A. Lacroix, Compt. Rend. Acad. Sci. Paris, 1910, vol. 151, p. 276.
[4] A. Lacroix, Min. France, 1909, vol. 3, p. 779.

Alumian and natroalunite.

The type material, the examination of which forms the subject of this paper, was collected by A. Breithaupt's son from three mines in the Sierra Almagrera, Southern Spain (37° 16′ N., 1° 47′ W.), and described by Breithaupt in 1858.[1] It is a decomposition product formed on pyrite and galena-bearing veins in an argillaceous schist and was accompanied by limonite. Breithaupt remarked that the mineral was composed of microscopic crystals, probably rhombs, that its density was 2·77–2·89 and that it consisted of alumina and sulphuric acid only, and gave to it the formula $Al_2(SO_4)_2O$.

Breithaupt's mineral has been re-examined optically and chemically and the cell dimensions have been determined from a powder photograph. The specimen (B.M. 92951) is a compact white piece with a few faint brown streaks (limonite) here and there. When scraped with a knife it yields a powder which if examined microscopically is seen to consist of minute rhombs (average size *c.* 10 μ). It was a matter of some difficulty to obtain ϵ but it is close to 1·590 and the mineral is optically

Table I. Chemical analysis and empirical unit-cell contents (rhombohedral cell) of alumian, together with other relevant data and the theoretical composition of natroalunite $NaAl_3(SO_4)_2(OH)_6$.

		Theoretical.	Cell contents.		
Na_2O	7·6	7·8	$Na^{\cdot}$	1·0	
K_2O	0·1		$K^{\cdot}$	—	D_4^{20} 2·780 ± 0·005
BaO	0·1		$Ba^{\cdot\cdot}$	—	
SrO	0·9		$Sr^{\cdot\cdot}$	—	R.I. (Na light)
PbO	0·6		$Pb^{\cdot\cdot}$	—	ϵ 1·590
Al_2O_3	36·8	38·4	$Al^{\cdot\cdot\cdot}$	2·9	ω 1·574
Fe_2O_3	0·4		$Fe^{\cdot\cdot\cdot}$	—	
SO_3	38·3	40·2	$SO_4^{\cdot\cdot}$	1·9	Cell dimensions (hexagonal axes)
H_2O^+	14·9	13·6	$OH^{\cdot}$	5·9	a 6·983 ± 0·002 Å.
H_2O^-	nil		H_2O	0·3	c 16·699 ± 0·002 Å.
	99·7	100·0			

positive. All relevant data are brought together in table I. The composition of the mineral shows that alumian is in fact the sodium end-member of the alunite series, a mineral so far unrecorded. The other data in the table confirm this statement. The water in the rhombohedral unit cell in excess of that demanded by the ideal composition for natroalunite is probably without significance, representing simply

water persistently retained owing to the finely divided state of the mineral.

Dept. of Mineralogy,
British Museum.

A. A. Moss

[1] Berg. hütten. Ztg., vol. 17, p. 53.

The nature of chlorospinel.

Chlorospinel was described in 1840 by G. Rose,[1] as a new grass-green variety of spinel from the Slatoust district, south Urals, characterized by the presence of considerable Fe_2O_3 and absence of FeO; two density determinations gave 3·591 and 3·594, in fair agreement with the densities calculated for the two analyses by H. Rose (table I, anals. 2 and 3) on the assumption (which is likely to be only approximately true) of a linear variation in density from $MgAl_2O_4$ 3·55 to $MgFe_2O_4$ 4·51: anal. 2, 3·63; anal. 3, 3·68. It has not been reported elsewhere and though it was synthesized by J. Morozewicz[2] no density or optical data were obtained on the synthetic material.

There are hardly any other original references to chlorospinel in the literature. N. Koksharov[3] states that it occurs 'in der Umgegend der Kussinsker Hütte' and both N. Koksharov[4] and P. Eremeyev[5] refer to its occurrence in chlorite-schist at the newly-discovered Praskovie-Evgenevsky mine, Shishimsk Mts., but the identification is not based on an analysis, and must be regarded as uncertain.

Recently N. G. Sumin,[6] confirming and extending work by L. L. Shilin,[7] has shown that two distinct green spinels occur in the Shishimsk area; one, occurring in ore-veins with chlorite and magnetite, has refractive index n 1·724 and was classified by Shilin as a common magnesium spinel; Shilin's analysis of the perovskite–magnetite–spinel ore shows it is not a zinciferous spinel, and its low refractive index suggests that it contains little FeO, so despite its green colour it cannot be classified with the ceylonites found elsewhere in the Slatoust region[3,4,5]. The second green spinel, from the chlorite-schist, has n 1·782, and agrees well in appearance and associations with Rose's chlorospinel; but an analysis by V. A. Moleva (table I, anal. 4), made on material in the Museum of the Academy of Sciences, U.S.S.R., collected in the first half of the nineteenth century, shows it to be a gahnospinel; Sumin therefore concludes that H. Rose's analyses were in error, and that his chlorospinel was in fact a gahnospinel.

TABLE I. New analytical, X-ray, and optical data for chlorospinel; together with other analyses of chlorospinel and of gahnospinel.

	1.		1.	2.	3.	4.	5.
MgO	26·5 %	Mg	7·8	7·8	8·2	4·5	5·3
FeO	1·8	Fe··	0·3	—	—	0·8	0·3
ZnO	0·8	Zn	0·1	0·04*	0·1*	2·7	2·8
MnO	0·3	Mn	0·05	0·06†	—	0·1	—
Al_2O_3	60·7	Al	14·1	14·8	13·5	15·3	15·7
Fe_2O_3	7·2	Fe···	1·1	1·3	2·2	0·6	—
TiO_2	1·2	Ti	0·2	—	—	0·04‡	—
Insol.	1·2	O	31·3	32	32	32	32
Sum	99·7	Sp. gr.	3·63	3·59		—	3·967

$D_{4°}^{24°}$ 3·63±0·01. n 1·729±0·002. a 8·105±0·005 Å.

* Cu. † Ca. ‡ Co.

1. Chlorospinel (B.M. 21993), Shishimsk Mts.; new analysis by D. I. Bothwell, and empirical unit-cell contents.
2–5. Atomic ratios to 32 oxygen.
2, 3. Chlorospinel, Shishimsk Mts.; G. Rose (H. Rose anal.), 1840.
4. Gahnospinel, Shishimsk Mts.; N. G. Sumin (V. A. Moleva anal.), 1955.
5. Gahnospinel, Ceylon; B. W. Anderson and C. J. Payne (M. H. Hey anal.), 1937; n_D 1·7465.

It seemed to us very unlikely that so competent an analyst as H. Rose should have failed to detect some 17 % of ZnO. Moreover, Sumin did not determine the density, which for a gahnospinel of this composition should be[8] between 3·9 and 4·0, against Rose's 3·59; and the refractive index should be around 1·76, against Sumin's 1·782 (apparently not on the material actually analysed).

We have therefore re-examined all the specimens of chlorospinel in the British Museum collections, and find all contain only small amounts of ZnO: B.M. 21993, from Shishimsk, bought of A. Krantz in 1848, has 0·8 % ZnO; B.M. 37185 and 37187, from Shishimsk, both from N. Koksharov's collection, have 1·4 % and 0·5 % respectively; and B.M. 89197, from the Slatoust region, acquired by R. P. Greg in 1850, has 0·8 %. A complete semimicro-analysis of B.M. 21993 was therefore made, together with refractive index and X-ray and density determinations on the material prepared for analysis. The results, included in table I, show that a third distinct green spinel occurs in the Shishimsk area besides green common spinel and Sumin's green gahnospinel; and this third spinel is G. Rose's chlorospinel, which was correctly analysed and is a valid variety.

Department of Mineralogy,
British Museum.

D. I. BOTHWELL
M. H. HEY

[1] G. Rose, Ann. Phys. Chem. (Poggendorff), 1840, vol. 50, p. 652.
[2] J. Morozewicz, Tschermaks Min. Petr. Mitt., 1898, vol. 18, p. 38.
[3] N. Koksharov, Min. Russlands, 1853, vol. 1, p. 211.
[4] Idem, ibid., 1866, vol. 5, p. 368.
[5] [P. Eremeyev] П. Еремѣевъ, Зап. Имп. Мин. Общ. (Verhandl. Russ. Min. Gesell.), 1869, new ser., vol. 4, p. 201.
[6] [N. G. Sumin] Н. Г. Сумин, Труды Мин. Муз. Акад. Наук СССР [Trans. Min. Mus. Acad. Sci. USSR], 1955, vol. 7, p. 161 [M.A. 13–189]. According to Sumin, the original discovery of chlorospinel by Bardot de Marin in 1833 was at the Praskovie-Evgenevsky mine; but Rose merely gives the locality as Slatoust, while Koksharov and Eremeyev, writing in the 1860's, describe this mine as 'newly discovered'.
[7] L. L. Shilin [Л. Л. Шилин], [Compt. Rend. (Doklady) Acad. Sci. URSS, 1940, vol. 28, p. 346]; abstr. M.A. 8–174.
[8] B. W. Anderson and C. J. Payne, Min. Mag., 1937, vol. 24, p. 547.

Mordenite, ptilolite, flokite, and arduinite.

Mordenite and ptilolite were first recognized as identical by Bannister[1] from a study of X-ray powder and rotation photographs. This observation was recorded in a footnote to a paper on heulandite by Hey and Bannister,[2] and was confirmed by Waymouth, Thornely, and Taylor,[3] who examined ptilolite from San Piero in Campo, Elba (B.M. 1914,321), mordenite from Aros, Isle of Mull (B.M. 47614), and type flokite (B.M. 1932,1297). They determined single crystal X-ray data for the Mull mordenite, but X-ray powder data were not recorded until 1954, when Harris and Brindley[4] gave results for the Mull mordenite above, together with cell dimensions derived from them. Dr. Hey has drawn attention to the fact that no X-ray data have hitherto been obtained on type specimens of mordenite or ptilolite, or on material from the type localities. This precaution is particularly desirable in view of the confused early history of mordenite.

Flokite[5] has also been recognized as identical with mordenite[1,3,6] and Bannister[7] has suggested that arduinite is impure mordenite. Stringham[8] compared arduinite from the type locality with a red zeolite from Tintic, Utah; he found that they gave identical X-ray powder patterns and optical data, but that both the unit-cell dimensions and the space group are the same as those of mordenite, and a chemical analysis of the Tintic material gave a composition near that of type mordenite.[9] Though Stringham had no authentic mordenite for comparison, he concluded that Billows' analysis[10] is in error, and arduinite is mordenite coloured by a little hematite.

Accordingly I have examined samples of all four species, namely: B.M. 43716, Mordenite, Morden County, Nova Scotia (type material

from Prof. How); B.M. 1932,1312, Mordenite (ptilolite), Green Mountain, Colorado (type locality); B.M. 1932,1297, Mordenite (flokite), Eskefjord (?), Iceland (type material); B.M. 1923,145, Mordenite (arduinite), Val de Zuccanti, Valdagno, Venetia, Italy (type locality).

Powder photographs were taken of the four specimens in a Phillips camera, 11·46 cm. diameter using Cu-$K\alpha$ radiation. The four photographs are identical as to line positions and show no significant variations in relative line intensities. Measured d-values agree with each other and with those listed by Harris and Brindley to within 0·1 %, except for the highest spacings, and the estimated relative intensities agree well with theirs. The results are therefore not repeated here and the data of Harris and Brindley can be accepted as applying to all varieties of mordenite.

The d-values for each photograph were assigned indices from the available unit-cell data[3,4,8] and examined for any systematic variation in cell dimensions. None was found, and the values obtained agree with those of Harris and Brindley within the limits of experimental error. The unit-cell volume is therefore 2800 ± 10 Å.^{3} for all mordenites, agreeing well with the value 2805 Å.^{3} calculated from the data of Waymouth *et al.*; Stringham's[8] value for arduinite, 2753 Å.^{3}, is not confirmed.

This constancy of the unit-cell dimensions of five mordenites from different localities contrasts with the variable composition of the mineral,[11] and supports the suggestion of Waymouth *et al.* that the structure is based on a rigid $(Si,Al)_{48}O_{96}$ framework.

I am grateful to Mr. D. L. Williams and Miss E. E. Fejer for help in taking and measuring the photographs.

R. J. Davis

Dept. of Mineralogy,
British Museum.

[1] F. A. Bannister, unpublished work, 1933.
[2] M. H. Hey and F. A. Bannister, Min. Mag., 1934, vol. 23, p. 559 n.
[3] C. Waymouth, P. C. Thorneley, and W. H. Taylor, ibid., 1938, vol. 25, p. 21
[4] P. G. Harris and G. W. Brindley, Amer. Min. 1954, vol. 39, p. 819 [M.A. **12**–486
[5] K. Callisen, Meddel. Dansk. Geol. For., 1917, vol. 5, no. 9 [M.A. **1**–23].
[6] O. B. Bøggild, K. Danske Vidensk. Selskab., Math. fys. Meddel., 1922, vol. no. 8 [M.A. **2**–59].
[7] F. A. Bannister, in M. H. Hey, Chem. Index of Minerals, 1st edn, 1950, entr 16.10.32.
[8] B. Stringham, Amer. Min., 1950, vol. 35, p. 601 [M.A. **11**–293
[9] H. How, Journ. Chem. Soc., 1864, vol. 17, p. 100.
[10] E. Billows, 1912; see Min. Mag., 1913, vol. 16, p. 353, and Dana, Syst. Min 6th edn, app. iii, p. 8.
[11] Dana, Syst. Min., 6th edn, pp. 572 and 573 (anal. 2 on p. 573 is of heulandite app. ii, p. 83; app. iii, p. 53; M.A. **1**–31, **2**–300, 301, **5**–162, **10**–37, 188, 297, 55 557, **11**–293, 550, **12**–84, 170, 486.